6-2022

Characterization of Larval Lepidopteran Gut Stem Cell Markers

Zilan Li
Clemson University, zilanl@g.clemson.edu

CHARACTERIZATION OF LARVAL LEPIDOPTERAN GUT STEM CELL MARKERS

A Thesis
Presented to
the Graduate School of
Clemson University

In Partial Fulfillment
of the Requirements for the Degree
Master of Science
Entomology

---

by
Zilan Li
August 2022

Accepted by:
Dr. Matt Turnbull, Committee Chair
Dr. Andrew Mount
Dr. Lisa Bain

ABSTRACT

The larval lepidopteran midgut is a complex tissue system that shows significant structure-function relationships related to its roles in digestive and absorptive processes. δ-endotoxins (Cry toxins) produced by the bacterium *Bacillus thuringiensis* disrupt the midgut epithelium of target insects has been used extensively to control pests. However, insects, including several lepidopteran species, evolve resistance to Cry toxins which causes a great threat to their continued utility. Understanding the physiology of the midgut, including that of the stem cells which are responsible for midgut growth, development, and regeneration, may improve the sustainability of midgut-targeted control like Cry toxins. Historically, lepidopteran midgut stem cells have been distinguished from mature cells by morphology, but this is unreliable due to significant morphological variation in both mature and stem populations, including during the differentiation processes of the latter. Thus, we examined three vital markers to distinguish larval lepidopteran midgut stem and mature cell types, as well as the differentiation state of stem cells using esterase activity (Calcein AM), mitochondrial density (Mitotracker), and mitochondrial membrane potential (TMRM). We also identified the existence and the expression level of one stemness maintainer gene Escargot among different development stages of lepidopteran larvae. Our results support the use of mitochondrial properties in lepidopteran midgut cell differentiation and indicate esterase activity is an insufficient marker even combined with morphology. Further, escargot transcript patterns support further examination of the role of the protein in gut physiology, including stem maintenance. Our results provide tools for

characterization and modification of physiological responses of lepidopteran midgut cells to stimuli and stresses. These in turn will aid in understanding conservation and divergence of developmental processes and development and use of pest control resources.

DEDICATION

To my mother and father, for always loving me and understanding my feelings.

ACKNOWLEDGMENTS

Foremost, I would like to offer my special thanks to my advisor Dr. Matt Turnbull, who helped me a lot in my research and gave me many useful suggestions. His support and patience built my confidence in my research life and guided me to be a real scientist. It's always a great pleasure talked with him during every meeting. He is role model that I would like to reach in future.

I also would like to thank Dr. Lisa Bain and Dr. Andrew Mount for being my committee members. The projects have been greatly improved with their help.

I also pay my sincere gratitude to my friends and colleagues. Thanks to Peng Zhang, Daniel Howard and Richard Melton for your assistance in my lab work. Thanks my best friend Yijie Gao for always supporting me and helping me keep a positive attitude. Thanks to my roommates and other friends for being my side.

Last, but not the least, my gratitude goes to my parents who are the most important inspiration for me.

TABLE OF CONTENTS

Page

LIST OF TABLES

LIST OF FIGURES

CHAPTER ONE

LITERATURE REVIEW

From embryogenesis to maturity, the formation of tissues and organs requires cells to proliferate and adopt different functions properly (Fuchs and Segre 2000). Once entering adulthood, many tissues and organs in the body engage homeostatic mechanisms to respond to natural cell death or injury, relying on cell replenishment. Many of these developmental and regenerative processes are based on stem cells. This type of cell owns outstanding abilities in maintaining the diversification of embryo, and development and regeneration of adult tissues and organs (Booth and Potten 2000, Fuchs and Segre 2000). However, relevant stem cell experiments are still limited by the lack of reliable markers when cells are in the steady state (Booth and Potten 2000, Bjerknes and Cheng 2005).

1. Stem Cells

Stem cells are undifferentiated cells with high plasticity and self-maintenance. They can proliferate or produce differentiated cells and switch between these two options when necessary (Booth and Potten 2000, Fuchs and Segre 2000, Marshman et al. 2002, Li and Xie 2005). The division of stem cells helps repair damage and maintain ongoing tissue homeostasis (Blau et al. 2001, Loza-Coll and Jones 2016). Both extrinsic signals and intrinsic programs maintain the properties of stem cells and their behavior in proliferation and differentiation (Blau et al. 2001, Li and Xie 2005).

Stem cells are mainly classified into embryonic stem cells (ESCs) and adult stem cells (ASCs) (Li and Xie 2005). ESCs originate from the inner cell mass (ICM) of the developing blastocysts (Chambers and Smith 2004, Young 2011). The pluripotency of

ESCs means they are able to differentiate into all three germ layers (ectoderm, endoderm, and mesoderm) and also produce progeny with the same genetic inheritance (Chambers and Smith 2004, Li and Xie 2005). The capacity of ESCs in pluripotency and self-renewal is maintained and regulated by several control factors in the genetic program of the organism (Young 2011).

Various ASCs are needed to develop organs post-embryonic development and the type is dependent on the tissue. ASC, such as the specific type of ASC in the intestine (Intestinal ASCs; ISCs), are essential to tissue homeostasis (Li and Xie 2005). Within each tissue, the well-organized microenvironment where stem cells locate is termed the stem cell niche (Li and Xie 2005, Resende and Jones 2012). The stem cell niche releases signaling molecules that regulate stem cell maintenance and proliferation, while the interaction between stem cells and niche cells also determines the size and occupancy of the niche (Li and Xie 2005, Losick et al. 2011, Korzelius et al. 2014). Different from ESCs, the potency of most ASCs in differentiation and regeneration is typically limited to the niche they inhabit, although some ASCs are highly plastic and can act outside of their niche (Blau et al. 2001, Li and Xie 2005). Several secreted ligand-receptor pathways regulating stem cell functioning have been studied and are covered below.

2. Intestine/Gut

The intestine is the largest immune organ in vertebrates and is one of the best models to study ASCs (Insoft et al. 1996, Sangiorgi and Capecchi 2008). The vertebrate intestine can be divided into the small and large intestines (MacDonald et al. 2011). The intestinal epithelium blocks the entrance of possible lethal substances effectively (Barker

2014). The intestinal epithelium also controls the flow of luminal contents into or out of the body, maintains the balance of digestion and absorption, and controls the occurrence of appropriate immune responses (Insoft et al. 1996, Apidianakis and Rahme 2011, Barker 2014).

The insect gut is structurally different from the vertebrate intestine, but there is similarity in morphological and physiological properties among different insect species (Engel and Moran 2013). The three major regions of the insect gut are the foregut, midgut, and hindgut, each with different functions in food ingestion and digestion (Corley and Mark 2006). The foregut and hindgut derive from the ectodermal cells and are covered with exoskeleton, while the midgut differentiates from endodermal tissues and is not lined with exoskeleton; the Malpighian tubules, located between the midgut and hindgut, are extensions of the anterior hindgut (Engel and Moran 2013). The foregut functions in transporting, storing, and processing ingested food (Takashima and Hartenstein 2012). The hindgut and the Malpighian tubules are primarily in charge of the osmoregulation of insects; the Malpighian tubules form the primary urine in the insects, while the hindgut reabsorbs the amino acids, water, and ions from the undigested food and waste, and produces the hyper- or hypo-osmotic urine (Engel and Moran 2013; Klowden 2013, Linser and Dinglasan 2014). The midgut, the longest section of the gut, is the primary site of nutrient absorption, digestion, and metabolization (Pauchet et al. 2008, Engel and Moran 2013).

The vinegar fly, *Drosophila melanogaster*, is an excellent model in the learning of intestinal stem cells (ISCs) formation and regulation, and its relevant research has been

and continues to be, applied to vertebrate intestinal study (Apidianakis and Rahme 2011, Takashima and Hartenstein 2012, Korzelius et al. 2014). For example, the cells and tissue of *D. melanogaster* and mammals are conserved sufficiently that some human pathogens are able to infect the former, enabling mechanistic studies of intestinal pathophysiology in a low-cost model (Apidianakis and Rahme 2011). Also, the responses of the *D. melanogaster* gut to injuries or infection can be used to assess the intestinal epithelial regeneration towards growth or immune factors (Apidianakis and Rahme 2011).

3. Intestinal/Gut Stem Cells

As noted, the vertebrate and insect intestines differ in structure, but the main cell classes are functionally similar (Apidianakis and Rahme 2011). The intestines of both groups contain secretory cells (referred to as goblet cells in insects), endocrine cells, enterocytes, and ISCs, but the locations of these cells differ across taxa. Both mammalian small intestine and adult fly midgut are maintained by ISCs, while the role of ISCs in the maintenance of *D. melanogaster* immature gut is unknown (Korzelius et al. 2014). ISCs in insects are morphologically and genetically similar to stem cells both in other insect niches and in other invertebrate and vertebrate taxa (Corley and Lavine 2006). Under the homeostatic state, ISCs will replenish themselves and differentiate into daughter cells (all types of mature intestinal epithelial cells) at a 1:1 ratio, while dividing symmetrically to produce two daughter cells after intestinal injury (Scoville et al. 2008, Korzelius et al. 2014).

Several factors and signaling pathways influence the formation and regulation of ISCs. There is high homology in these same signaling pathways among the mammalian

and insect intestines (Scoville et al. 2008, Apidianakis and Rahme 2011, Takashima and Hartenstein 2012). Wnt protein in intestines, which promotes the renewal of ISCs in both groups, is produced by myofibroblasts and Paneth cells in vertebrates, and produced by visceral muscle cells in *D. melanogaster* (Takashima and Hartenstein 2012). The function of Notch signaling in ISC programming also is conserved between mice and flies: Notch manages the balance of self-renewing stem cells and differentiated daughter cells, as activation of the Notch pathway leads to the differentiation of *D. melanogaster* ISCs, while the absence of Notch signaling decreases the proliferation of stem cells (Takashima and Hartenstein 2012). It remains unclear how pluripotency in vertebrate ISCs is derived from embryonic progenitors. However, in *D. melanogaster*, it is clear that a small number of embryonic progenitors in the larvae are maintained through larval-pupal molts and pupal-adult metamorphosis and become adult ISCs (Takashima and Hartenstein 2012). The degree of evolutionary conservation in ISC biology between fly and mammals, along with the available knowledge for *D. melanogaster*, suggests that fly may serve as a great model to better understand ISC regulation in other insects for which regulation of ISCs is unclear, including lepidopterans.

4. Lepidopteran Midgut Stem Cells

The insect order Lepidoptera (moths and butterflies) is one of the most widespread insect groups on Earth, and their herbivorous larvae may be tremendous pests (Linser et al. 2014, Wu et al. 2016). The efficient ability of lepidopteran insects in food digestion, nutrient absorption, and immune responses through the midgut play important roles in their evolutionary success (Zhang et al. 2011, Engel and Moran 2013, Wu et al.,

2016). The midgut produces critical proteins which assist the digestibility of host plant material, but also help lepidopterans detoxify ingested toxic compounds and pathogens (Pauchet et al. 2008, Zhang et al. 2011, Wu et al. 2016). Correspondingly, lepidopterans are susceptible to control through the interference of these characters, such as through ingestion of pathogenic microbes, plant toxins, bacterial-derived cry toxins, and synthetic insecticides.

The lepidopteran midgut is a single-layer epithelium comprised of four types of cells: goblet cells, columnar cells, endocrine cells, and stem cells. They are historically distinguished by morphology. The columnar cells are the most abundant cell type, with brush-like borders that contain numerous microvilli and folds on the apical surface of the membrane, which increases the surface area for food digestion and nutrient absorption (Zhang et al. 2011, Klowden 2013). The central chalice-shaped cavity formed by invagination of the apical surface is the characteristic morphological property of goblet cells, which are distributed through the epithelium (Santos et al. 1984, Klowden 2013, Wu et al. 2016). The K^+ pump on the apical surface of goblet cells regulates the ion balance in the gut by generating H+ and K+ gradients, thus influencing water movement; transportation of cell debris and metabolization of gut components also occurs inside goblet cells (Gomes et al. 2013, Klowden 2013, Wu et al. 2016). Additionally, a small number of endocrine cells arise at the base of columnar cells (Santos et al. 1984, Klowden 2013). These cells are responsible for the integration of food digestion and endocrine systems, assessment of food, and information transmission (Klowden 2013). However, relatively little is known regarding the enteroendocrine system in

lepidopterans. All three types of cells mentioned above are terminally differentiated cells in the gut.

Gut, or intestinal, stem cells are scattered among the bases of the epithelial cells or exist among the mature cells during differentiation in the larval molting period (Corley and Lavine 2006, Loeb et al. 2003). Gut stem cells are the only cell type in the lepidopteran larval gut that undergo mitosis to proliferate, and also are the only cell type capable of differentiating into other cell types during gut development or repair following injury (Loeb and Hakim 1996, Hakim et al. 2001, Loeb et al. 2003, Castagnola and Jurat-Fuentes 2016, Caccia et al. 2019). The proliferation and differentiation processes balance the number of stem cells and provide new columnar, goblet, and endocrine cells to maintain the physiological stability of the gut (Castagnola et al. 2011). However, midgut stem cells are difficult to distinguish from endocrine cells due to their similar shapes, as both are small and round, and there is a lack of empirically supported markers for both cell types.

δ-endotoxins (Cry toxins) produced by the bacterium Bt exhibit insecticidal activity (Bretschneider et al. 2016). Transgenic plants that express Bt-Cry toxins have been widely adopted agriculturally and their use has significantly reduced the use of chemical insecticides (Bretschneider et al. 2016, Bravo et al. 2007). These proteins kill lepidopteran pests primarily by lysing larval lepidopteran midgut epithelial cells (Tabashnik 1994, Bravo et al. 2007, Tabashnik et al. 2013). However, numerous species of lepidopterans have demonstrated the capacity to evolve resistance toward Cry toxins in the lab and field, threatening their effectiveness in pest control (Tabashnik 1994, Heckel

et al. 2007, Tabashnik et al. 2013). Several mechanisms of resistance have been identified, including reduced Cry toxin activation and altered receptor availability and binding (Bravo et al. 2007, Bretschneider et al. 2016, Liu et al. 2021). Additionally, while most resistance mechanisms identified thus far affect the activation and binding of the Cry proteins, other mechanisms like behavioral avoidance may also cause reduced Cry toxin efficacy (Rausell et al. 2004, Bilbo et al. 2019).

Several studies have also suggested that midgut epithelium dynamics may affect resistance to Cry toxins and other damaging stimuli. Following treatment with sublethal doses of two strains of Bt Cry toxin (AA 1-9 and HD-73), the number of stem and differentiating cells (identified morphologically) in cultured midgut cells from the pest lepidopteran *C. virescens* (previously *Heliothis virescens*) increased compared with controls, while the number of columnar and goblet cells decreased relative to controls (Loeb et al. 2001). The mortality of baculovirus-infected larvae was also connected with the sloughing (removal) of infected midgut cells and subsequent epithelial cell replacement (Hoover et al. 2000). Together, these results imply that damage-induced loss of mature cells may stimulate midgut stem cell division and differentiation (Loeb et al. 2001). Additionally, *C. virescens* gut stem cells, identified by morphology, differentiated and proliferated when cultured with fetal bovine serum and Albumax II (a mammalian ESC media additive), respectively (Castagnola and Jurat-Fuentes 2016). Such studies examining regulation of lepidopteran gut stem cells, including their origin, maintenance, and differentiation, would be furthered by the development of reliable markers for their identification (Corley and Lavine 2006). This in turn could further help understand

lepidopteran midgut epithelial development and regeneration, thus being helpful for insect control (Hakim et al. 2001). However, the absence of reliable markers for midgut stem cells limits such studies. Lepidopteran midgut cells have been historically distinguished from mature cells by morphology, but as noted above, this is unreliable as stem cells are morphologically similar to endocrine cells, and the former colocalize with the latter in some cases (Bjerknes and Cheng 2005, Castagnola et al. 2011, Zhou et al. 2019).

5. Lepidopteran Gut Stem Cells Markers

Calcein acetoxymethyl ester (calcein AM) has previously been used in a number of taxa and stem cell lineages to discriminate stem from terminally-differentiated cells. It is a non-fluorescent compound that is cell membrane permeable and is often used to detect cell viability (Allen et al. 2009, Chu and Sam 2009). Nonspecific intracellular esterases cleave the calcein AM, producing calcein, generating fluorescence emission in the cytosol without dye binding to DNA (Allen et al. 2009, Chu and Sam 2019). Calcein AM is non-toxic and is not known to change cell physiology, for example, both during and subsequent to calcein AM exposure, cancer stem cells (CSCs) maintained the same proliferation ability and viability as unstained controls (Allen et al. 2009).

Calcein AM has been used to identify presumptive lepidopteran larva gut stem cells previously. In *C. virescens*, midgut-derived cells morphologically identified as stem cells exhibited more intense calcein AM emission than mature cells, leading the study authors to propose that the former population has higher esterase activity and/or reduced calcein AM efflux than the latter (Castagnola et al. 2011). Similar results were obtained

with *Spodoptera litura* in which gut cells identified by morphology as probable stem cells showed higher calcein AM emission than mature cells, a result explained as being due to the former expressing higher esterase activity (Pandey and Rajagopal 2017). In larval midgut cells of the lepidopteran *Chilo suppressalis*, mature cells with lower calcein AM fluorescence were distinguished from postulated stem cells with higher calcein AM fluorescence, but stem cells undergoing differentiation could not be distinguished from mature cells by calcein AM (Zhou et al. 2019). Thus, neither morphology nor calcein AM alone, nor in combination, appear sufficient to discriminate stem cells from endocrine cells, nor stem cell differentiation status.

Mitochondria are membrane-bound organelles that provide chemical energy for cells through the production of adenosine triphosphate (ATP) (Parker et al. 2009, Sukumar et al. 2016). The function and integrity of mitochondria may affect stem cell viability, proliferation and differentiation potential, and lifespan (Parker et al. 2009, Ye et al. 2011). The nature of mitochondria determines in part the ability of somatic stem cells to regulate Reactive Oxygen Species (ROS) and oxidative stress response, and this further determines the proliferative and differentiation fate of the cells (Parker et al. 2009). Mitochondrial membrane potential ($\Delta\Psi_m$) is the electrical potential difference between the matrix and the cytosol of mitochondria (Scaduto and Grotyohann 1999, Ly et al. 2013). Recent studies have demonstrated that the fate of stem cells may be influenced by mitochondrial state including $\Delta\Psi_m$ and overall metabolic activity (Table 1). For example, reducing $\Delta\Psi_m$ enhanced hematopoietic stem cell (HSC) function (Mantel et al. 2010). However, caution must be taken in interpreting $\Delta\Psi_m$ as a marker for stem cells.

For example, there are both low and high $\Delta\Psi_m$ populations of mouse ESCs, and while they exhibit different metabolic rate, they are morphologically indistinguishable and exhibit equivalent pluripotency (Schieke et al. 2008).

Mitochondrial mass (load or number) differs both within and between cell types, as it is tied to cell state; in stem cells, mitochondrial mass has been connected with the proliferation process and ATP synthesis (Lee et al. 2002). Also, de Almeida et al. (2017) proposed that HSCs had higher mitochondrial mass than mature cells and the mitochondrial mass decreased during the differentiation of HSCs, and Liu et al. (2019) stated that that human dermal stem cells (hDSCs) contained very numerous mitochondria.

Few studies have reported both the $\Delta\Psi_m$ and mitochondrial mass of stem cells together, but considering the above, the situation may be that $\Delta\Psi_m$ and mitochondrial mass are inversely proportional in stem cells with high mitochondrial mass and low $\Delta\Psi_m$ predicted. Characterization of both $\Delta\Psi_m$ and mitochondria mass may thus serve as a reliable indication of larval lepidopteran midgut stem cells versus mature cells, would fill in a gap in the mitochondrial information of insect midgut stem cells, and may serve to discriminate multiple states of gut stem cells.

Besides using non-invasive and non-toxic dyes to differentiate stem cells in different tissues, several specific genes or proteins related to stem cell identification have also been applied (Barker 2014). The neural RNA-binding Musashi homologue 1 (Msi1) protein maintains the neural stem cells and is considered a potential marker in mouse neural stem cell identification (Sakakibara et al. 1996). Msi1 also is present where ISCs are localized and in the crypt base columnar cells (Kayahara et al. 2003). Besides Msi1,

Lgr5 also is suggested to potentially serve as a marker of mouse crypt base columnar (CBC) stem cells, and Prominin 1 (Prom1) is a marker of CSCs (Barker et al. 2007, Barker 2014). The mammalian Snail family members have been proposed to regulate stem cell fate through undetermined mechanisms (Korzelius et al. 2014). In *D. melanogaster* midgut, ISCs express the Snail homolog *escargot* (*esg*), which maintains the stemness status of those cells (Korzelius et al. 2014). The presence and role of esg in *D. melanogaster* midgut stem cells along with the role of Snail homologues in mammals suggests its utility as a phylogenetically conserved stem cell marker. However, no esg homologue has been reported or studied in lepidopterans.

The objectives of the proposed study here were to develop reliable markers for the detection and subsequent study of lepidopteran midgut stem cells. We characterized and integrated the esterase activity, mitochondrial membrane potential, and mitochondrial mass of midgut cells in immature Lepidoptera. The vital markers used will improve our ability to identify, characterize, and isolate lepidopteran midgut cells. We also isolated an escargot homologue from the lepidopteran *C. virescens* and characterized its expression level at different stages of immature development. Based on our two objectives, my data provide the ability to study further and better understand lepidopteran midgut stem cells, and to develop modifiers of their activity.

Table 1 Mitochondrial membrane potential and mitochondrial mass of stem cells and their derivatives in different systems. NR = Not Reported

Cell types	Characteristics	Mitochondrial Membrane Potential ($\Delta\Psi_m$)	Mitochondrial mass
Human Hematopoietic Cell	Hematopoietic Stem Cell (HSC)	Low	High
	Hematopoietic Terminal/ Differentiating Cell	High	Low
Human Dermal Stem Cell (hDSCs)		One group showed high $\Delta\Psi_m$, one group showed low $\Delta\Psi_m$	High
Human Breast cell/Cancer Cell	Metastatic Breast Cancer Stem Cell (CSC)	NR	High
	Breast Cell	NR	Low
	Embryonic Stem Cells (ESCs)	NR	High
	Differentiated ESCs	NR	Low
Mouse Embryonic Stem Cells		Low $\Delta\Psi_m$, high resting $\Delta\Psi_m$	NR

CHAPTER TWO

DISTINGUISHING LARVAL LEPIDOPTERAN MIDGUT CELLS USING VITAL MARKERS

1. Abstract

The larval lepidopteran midgut is a complex system that shows significant structure-function relationships related to its roles in digestive and absorptive processes. Understanding the physiology of the midgut, including the stem cells which are responsible for its growth, development, and regeneration, may improve the sustainability of midgut-targeted controls. Historically, midgut stem cells have been distinguished from mature cells by morphology, but this is unreliable due to significant morphological variation in both mature and stem populations, including during the differentiation processes of the latter. Thus, we are examining vital markers to distinguish larval lepidopteran midgut stem and mature cell types using esterase activity (calcein AM), mitochondrial density (Mitotracker), and mitochondrial membrane potential (TMRM). Our data confirm the usability of mitochondrial properties and raise concerns over the reliability of esterase activity to distinguish midgut stem and mature cells. Combined with advanced techniques like flow cytometry, future studies may use these markers to better study developmental and physiological responses of lepidopteran gut cells to stimuli and stresses.

2. Introduction

The order Lepidoptera (moths and butterflies) is one of the most widespread insect taxa on Earth, and their larvae are tremendous pests, annually causing severe losses in agricultural crops globally (Linser et al. 2014, Wu et al. 2016). The impressive functionality of the lepidopteran midgut in digestive, absorptive, metabolic, and immune systems contributes to their ecological success (Zhang et al. 2011, Engel and Moran 2013, Wu et al. 2016). The lepidopteran larval midgut comprises four types of cells, which can be categorized into terminally-differentiated/mature cells (goblet, columnar and endocrine cells) and stem cells. The columnar cells with brush-like borders are mainly responsible for food digestion and nutrient absorption (Cioffi 1979, Loeb 2010, Zhang et al. 2011), while the cup-shaped goblet cells regulate ion movement by generating H+ and K+ gradients (Dow 1992, Loeb 2010, Gomes et al. 2013, Wu et al. 2016). Goblet cells also function as a depot where the transportation of cell debris and metabolization of midgut components occurs (Gomes et al. 2013). The less-studied endocrine cells integrate digestive and endocrine systems by releasing peptides (Caccia et al. 2019).

Stem cells are responsible for cell replenishment in the midgut. In general, the midgut stem cell produces one daughter stem cell and one daughter cell that keeps differentiating into mature cells (Booth and Potten 2000, Korzelius et al. 2014). Seldomly, a stem cell performs symmetrical division by producing two stems or two mature cells (Booth and Potten 2000). The tissue environment may account for the forms of stem cell division, for example, stem cells divide symmetrically after intestinal injury

(Booth and Potten 2000, Scoville et al. 2008). The proliferation and differentiation of stem cells ensure midgut growth, maintain midgut stability, and repair the injured midgut.

δ-endotoxins (Cry toxins) produced by the bacterium *Bacillus thuringiensis* (Bt) exhibit insecticidal activity in lepidopteran pests primarily by lysing larval midgut epithelial cells (Tabashnik 1994, Bravo et al. 2007, Bretschneider et al. 2016). Stem cells have been shown to play a critical role in recovering midgut epithelium from Cry toxin intoxication, as well as other damaging stimuli (Loeb et al. 2001). After treating cultured larval midgut cells of the noctuid *C. virescens* with sublethal doses of two strains of Bt Cry toxin (AA 1-9 and HD-73), numbers of resting stem cells and differentiating cells (stem cells in differentiating state which develop into mature cells) increased compared with untreated controls, while columnar and goblet cells decreased relative to controls (Loeb et al. 2001). Similarly, newly differentiated midgut cells were observed along with swollen and lysing columnar cells following Bt infection in larvae of the pyralid *Corcyra cephalonica* (Chiang et al. 1986).

Identifying undifferentiated midgut stem cells among larval stages of insects is necessary to better understand their origin, maintenance, and differentiation (Corley and Lavine 2006). This could clarify aspects of midgut epithelial development and regeneration, thus being helpful for controlling larval resistance toward Bt or other insecticides. However, the lack of specific and reliable markers for lepidopteran midgut stem cells hinders this progress. Midgut mature cells and stem cells have historically been distinguished by morphology. This is unreliable as midgut stem cells are difficult to distinguish from endocrine cells due to their similar shapes, as both are small and round

(Bjerknes and Cheng 2005). In theory, culturing primary stem cells could help identify stem cells according to their proliferation and differentiation ability. However, culturing stem cells is technically difficult, and the lack of markers would preclude the characterization of stem cell response to the stimulus. Additionally, some endocrine cells colocalize with stem cells at the basal epithelia, reducing the utility of location for discrimination (Levy et al. 2004, Bjerknes and Cheng 2005, Pinheiro et al. 2008).

Numerous studies have examined the suitability of mitochondria in distinguishing SC from terminally differentiated cells. Here, the assumption is that as cell function changes, metabolic demands and thus mitochondrial activity change. Therefore, stem and mature cells are hypothesized to differ in mitochondrial characteristics. Two properties of mitochondria, mitochondrial membrane potential ($\Delta\Psi_m$) and mitochondrial mass, have been used in identifying mammalian stem cells. Self-renewing HSCs exhibit reduced $\Delta\Psi_m$ (depolarized mitochondria) relative to mature cells (Schieke et al. 2008, Sukumar et al. 2016). However, this is not consistent across stem cell systems and caution needs to be taken when using $\Delta\Psi_m$ as a marker for stem cells. In mouse ESCs and human dermal stem cells (hDSCs), both low and high $\Delta\Psi_m$ stem cell populations are observed. The different $\Delta\Psi_m$ populations of both ESCs and hDSCs are morphologically indistinguishable and exhibit equivalent pluripotency, but have different metabolic rates (Schieke et al. 2008, Liu et al. 2019). Stem and mature cells may also exhibit different mitochondrial content. For example, higher mitochondrial mass is exhibited in HSCs and hDSCs, while during HSC differentiation, mitochondrial mass decreased (de Almeida et al. 2017, Liu et al. 2019).

Intracellular esterase activity may also differ in stem and terminally differentiated cells, enabling the distinction of these cells by the esterase-activated fluorescent dye calcein AM dye (Allen et al. 2009, Chu and Sam 2009, Castagnola et al. 2011, Pandey 2017, Zhou et al. 2019). In mammals, live putative CSCs have successfully been distinguished from non-CSCs of the tumor by calcein AM staining (Allen et al. 2009). Differential calcein AM fluorescence has also been proposed to differentiate stem cells from mature cells in lepidopteran larval midguts. Small midgut cells from *C. virescens*, hypothesized to be stem cells, exhibited higher calcein AM fluorescence intensity than larger cells, presumably due to the former having either higher esterase activity, or mature cells exhibiting greater calcein AM efflux (Allen et al. 2009, Castagnola et al. 2011). A similar difference in calcein AM intensity was also observed between presumptive midgut stem cells and mature cells in both *C. suppressalis* and *S. litura* (Pandey 2017, Zhou et al. 2019).

Given the above, it is apparent that single characteristics (e.g., morphology, location, esterase activity) may be insufficient to distinguish lepidopteran larval midgut stem from mature cells. Therefore, to distinguish cell populations from the midgut of larval *C. virescens*, we examined the suitability of mitochondrial markers in combination with the use of the previously used morphology and esterase activity (calcein AM). In addition to determining the patterns of $\Delta\Psi_m$ and mitochondrial mass in midgut cells and their correlation to previous identifying characteristics, examination of $\Delta\Psi_m$ and mitochondria mass further will fill in a gap in the mitochondrial information of insect midgut stem cells.

2. Materials and Methods

2.1 Insects

Second and third instar *C. virescens* (Lepidoptera: Noctuidae) larvae were obtained from Benzon Research (Carlisle, PA). Larvae were reared on an artificial diet supplied with the larvae and maintained at room temperature. Head capsule slippage was used to time larva molting and new stage development (Capinera 2012), and 4^{th} instar larvae were used in the midgut dissection.

2.2 Midgut dissection and midgut cell isolation

To isolate gut cells for subsequent analysis, six 4^{th} instar *C. virescens* larvae were anesthetized on ice for 5mins. Before dissection, the surface of the larvae was sterilized by brief immersion in a sterile washing solution (3% Dawn liquid dish detergent + 30% sterile distilled-deionized water + 67 % Clorox bleach). Midgut dissection was immediately performed after transferring the larva onto a wax dissection plate containing sterile Ringer's solution (137 mM NaCl, 1.8 mM $CaCl_2$, 2.7 mM KCl, 2.4 mM $NaHCO_3$) (Castagnola et al. 2011). The larval head and telson were immobilized with sterile dissection pins, then the entire dorsal midline was cut from the posterior to the anterior. Gut contents, peritrophic membranes, and the Malpighian tubules were cleaned from the larval midgut by sterile dissection scissors. The excised midgut was rinsed briefly in 3mL sterile Ringer's solution. Washed midguts were minced and incubated in 3mL fresh incubation media (1:3 sterile Ringer's: rest supplemented Grace's insect Media, 15 µM gentamicin, 1X antibiotic/antimycotic) for 90 minutes at room temperature. Tissue

fragments then were homogenized gently in the incubation media by trituration with a pipette and transferred to a 70μm cell strainer (Thermo Fisher Scientific, MA) in a sterile 15mL conical tube. The tube was centrifuged (400g) for 5 minutes at 4°C. The supernatant was discarded, and the pellet containing the midgut cells was resuspended in 3mL incubation media with suitable vital makers.

2.3 Vital staining of midgut cell cultures

Two combinations of vital markers were used to stain the midgut cell cultures. Calcein AM Green (Invitrogen, CA) and Tetramethylrhodamine methyl ester red (TMRM) (Anaspec, CA) were used to fluorescently stain midgut cell intracellular esterase activity and mitochondrial membrane potential ($\Delta\Psi_m$), respectively. Alternatively, midgut cells were double-stained with MitoTracker Green (MTG) (Invitrogen, CA), labeling mitochondria, and TMRM. Dyes were thawed on ice and added to cells at final concentrations of 500nM (calcein AM), 200nM (TMRM), and 200nM (MTG) in 3mL incubation media. Dye incubation was performed at room temperature for 30 mins and protected from light. At the end of this incubation period, tubes were centrifuged (400g) for 5 mins at 4 °C, and the supernatants were discarded. The stained pellet was gently resuspended with 1 mL fresh incubation media and transferred into a 6-well plate for fluorescence observation.

2.4 Fluorescence analysis

Cells were imaged with a monochromatic DS-QiMc camera (Nikon) on a TE2000 epifluorescence microscope (Nikon). FITC (Ex: 460-500, Em: 510-560) and TRITC (Ex: 530-560, Em: 590-650) filters were employed to measure the fluorescence. Before capturing images of cells, one image without an excitation light source was captured ("ambient light value", or DF) with NIS-Elements BR 2.3 software, and the ambient light value was later measured in FIJI (version 1.0). One brightfield image and two single-channel fluorescence (FITC and TRITC channels) images were captured for the same region of interest and stacked in FIJI. Big and small cells in equal numbers were selected haphazardly and outlined manually in the brightfield image, and area, perimeter, and mean gray value (intensity) were only measured on the fluorescent layers. Data from FIJI were transferred to Microsoft Excel for data management.

2.5 Data management and statistical analysis

Five random regions of the DF image (no excitation light) were selected and their average 'mean gray value' was considered as ambient light value (DF) (Zhang and Turnbull 2018). For each fluorescent image, the average 'mean gray value' of five background regions without cells was used as background fluorescence (FF). The background fluorescence (FF) value and ambient light value (DF) were used to normalize the mean intensity of each cell, using the following equation:

Normalized intensity (NF) = (Mean intensity-DF)/(FF-DF)

The circularity of each cell was generated using the following equation:

$$\textbf{Circularity} = (4 \times \pi \times \textbf{Area}) / \textbf{Perimeter}^2).$$

Eight independent replications of the TMRM and MTG staining were performed, while TMRM and calcein AM staining had five independent replications. In each replicate, the means of NF, circularity, and area of each big and small cell pool were calculated. For replications of TMRM and MTG staining, TMRM NF was further normalized by MTG NF.

The normalized TMRM of each cell was generated using the following equation:

$$\textbf{Normalized TMRM} = \textbf{TMRM NF/MTG NF}$$

The distribution of the pooled means was then analyzed statistically. Normality of distribution and homogeneity of variance were tested in R Studio (v1.4.1106) using Shapiro-Wilk and Levene's tests, respectively, then tested for significant differences ($\alpha = 0.05$) using t-test or ANOVA with post-hoc Tukey's test (JMP, v16.0). Figures were generated in JMP (v16.0).

3. Results

3.1 Morphology of Chloridea virescens *midgut cells*

Different classes of morphologies of cells were initially observed in the *C. virescens* midgut cell culture based on gross cell morphology, obvious to visual inspection (Fig. 1A). Cells with large areas typically also had irregular shapes; collectively, these are referred to here as Large Irregular Cells (LICs). Similarly, cells with smaller areas generally had round shapes, and are referred to here as Small Round Cells (SRCs). Among LICs, columnar cells ("enterocytes") exhibit columnar shapes with large cell areas and brush-like borders (Fig. 1A). LICs also include notable goblet cells, which have obvious central chalice-shaped cavities formed by membrane invagination and larger cell areas (Fig. 1A). SRCs are likely a mixed population of stem and endocrine cells (Endo and Nishiitsutsuji-Uwo 1981, Bjerknes and Cheng 2005).

Area and circularity were examined for SRCs and LICs following staining with either vital dye pairing (CAMG+TMRM, MTG+TMRM). Following CAMG+TMRM staining, mean area (± standard error) of LICs and SRCs were 677.66 ± 25.60 μm^2 and 46.86 ± 4.57 μm^2, which significantly differed [t (4.25) = -24.56, $P < 0.001$] (Fig. 1B). Mean area of LICs and SRCs stained with MTG+TMRM were 667.61 ± 26.23 μm^2 and 53.83 ± 5.89 μm^2, respectively, which also significantly differed [t (7.7) = -22.83, $P < 0.001$] (Fig. 1B). Likewise, mean Circularity values for LICs (0.80 ± 0.01) and SRCs (0.92 ± 0.02) stained with CAMG+TMRM significantly differed [t (7.93) = 7.90, $P < 0.001$], as did the mean Circularity values for LICs (0.82 ± 0.01) and SRCs (0.94 ± 0.00) stained with MTG+TMRM [t (9.04) = 12.57, $P < 0.001$] (Fig. 1C).

A

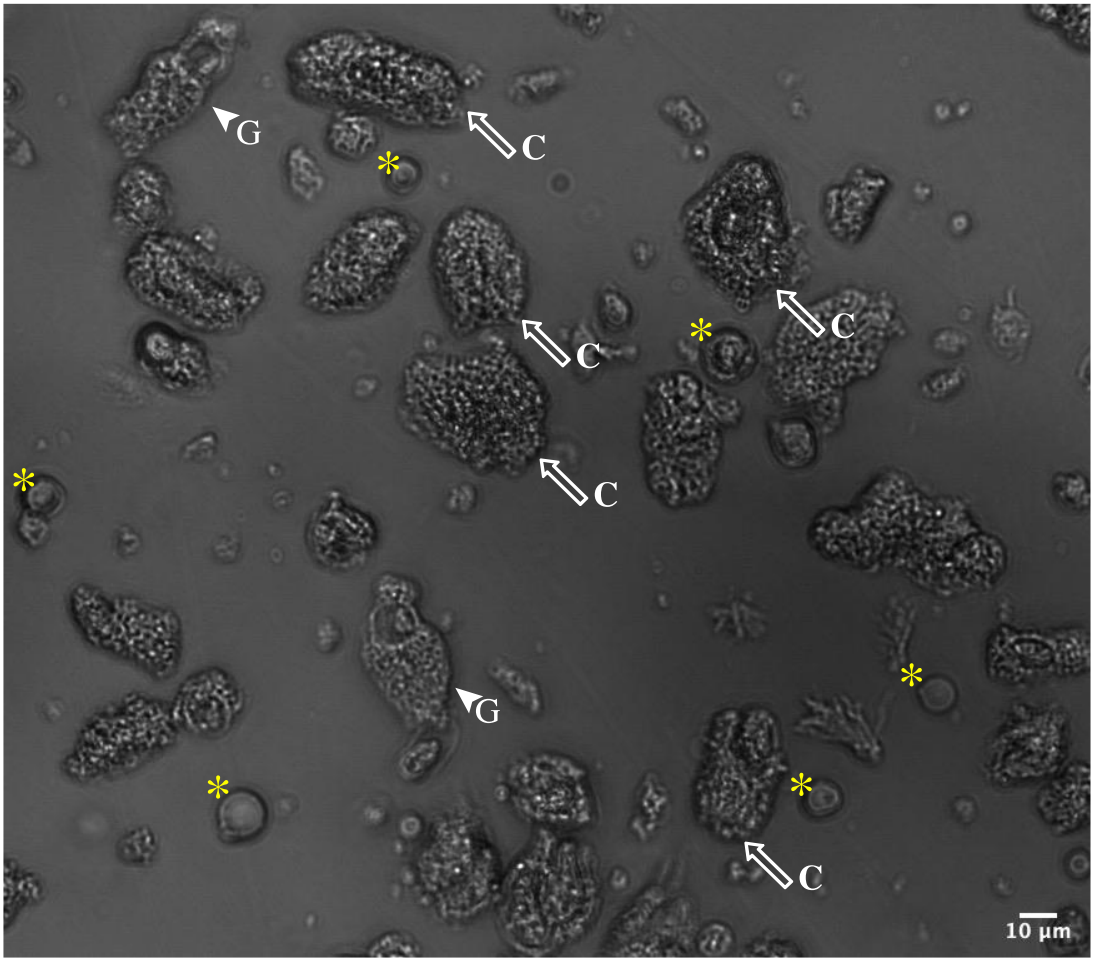
G
C
C
C
C
G
C
10 µm

B

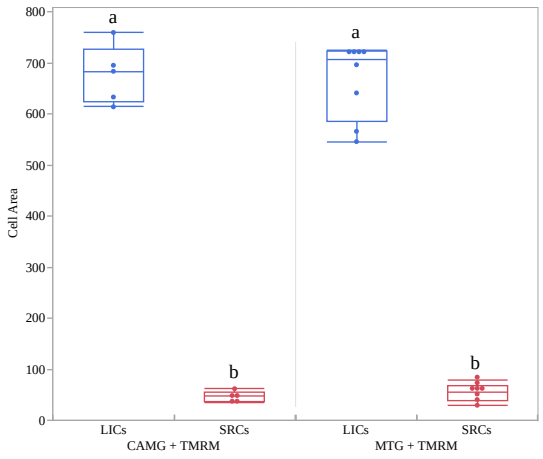
Cell Area
800
700
600
500
400
300
200
100
0
a
b
a
b
LICs
SRCs
LICs
SRCs
CAMG + TMRM
MTG + TMRM

C

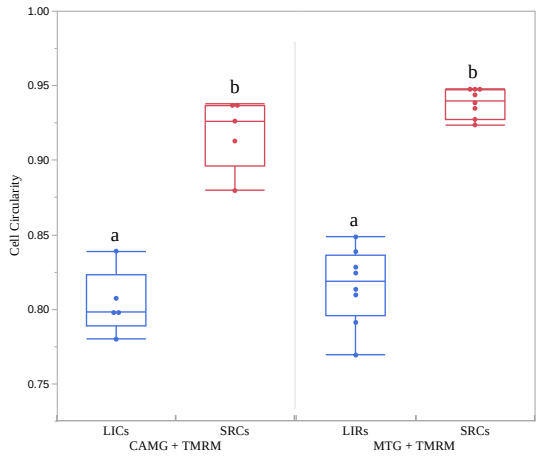
Cell Circularity
1.00
0.95
0.90
0.85
0.80
0.75
a
b
a
b
LICs
SRCs
LIRs
SRCs
CAMG + TMRM
MTG + TMRM

Figure 1. Morphology of mixed *C. virescens* larval midgut cells. (A) LIC and SRC populations are shown. Columnar cells are marked with white arrows. Goblet cells are marked with white arrowheads. SRCs are marked with yellow asterisks *. Different arrows point to specific SRCs: C = columnar cells, G = goblet cells. Scale bar = 10μm. (B) Area of LICs and SRCs stained with CAMG + TMRM (left panel) and MTG + TMRM (right panel). (C) The circularity of LICs and SRCs stained with CAMG + TMRM (left panel) and MTG + TMRM (right panel). Statistical significant difference between LIC and SRC populations within the staining regime is marked by different letters above each column (*t*-test, $P < 0.001$).

3.2 Separation and characterization of C. virescens *midgut cell cultures using calcein AM and TMRM*

Subsequent to outlining LICs and SRCs in the brightfield layer and determining area and circularity, ROIs were analyzed for grey-scale value (fluorescence emission) for calcein AM and TMRM. Values collected represented the mean pixel intensity for each ROI. Mean calcein AM values (LIC=4.55 ± 0.87, SRC=2.85 ± 0.37) did not differ between LICs populations and SRCs populations [t (5.41) = -1.79, P = 0.13] (Fig. 2A).

To more accurately differentiate LICs and SRCs, they were also characterized by TMRM fluorescence, which reflects mitochondrial membrane potential ($\Delta\Psi_m$). Mean TMRM fluorescence in the LICs (10.67 ± 2.45) was significantly higher than in the SRCs (2.77 ± 0.16) [t (4.04) = - 3.22, P = 0.032] (Fig. 2B), indicating that LICs had higher $\Delta\Psi_m$ (that is, they are more hyperpolarized).

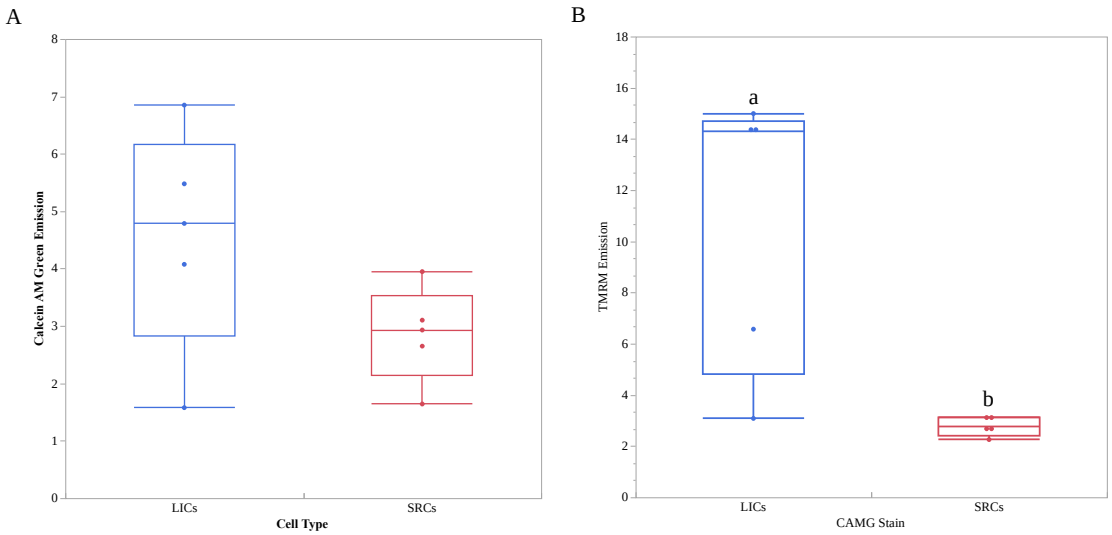

Figure 2. Fluorescence intensities of mixed *C. virescens* larval midgut cells population co-stained with calcein AM and TMRM. (A) The esterase activities of LICs and SRCs were measured by calcein AM. The esterase activity did not differ within the two cell populations. (B) Mitochondrial membrane potential, as measured by TMRM fluorescence emission, of LICs and SRCs significantly differs.

3.3 Separation and characterization of C. virescens *midgut cell pools using MTG and TMRM*

TMRM emission values were measured by total TMRM fluorescence standardized to the cell area in FIJI, which means the TMRM fluorescence intensity would be affected by the mitochondrial numbers inside of cells. In part to control for this, cells were co-stained with MTG. MTG represents the mitochondrial mass of cells, providing information on differential mitochondrial densities among cell types, as well as permitting normalization of TMRM value.

Midgut LICs incubated with TMRM + MTG had a mean TMRM value (8.39 ± 1.90) that was significantly higher than that of SRCs (2.08 ± 0.23) [t (7.20) = -3.30, *P* = 0.01] (Fig. 3A). When measuring the MTG fluorescence emission in the midgut cell

cultures, there was a significant reduction in the SRC population fluorescence (1.86 ± 0.19) as compared to LIC (2.62 ± 0.26) [t (12.89) = -2.38, P = 0.03] (Fig. 2C), indicating SRCs have a lower mitochondrial count than LICs.

After normalization with MTG, TMRM fluorescence of SRCs (1.28 ± 0.14) was significantly lower than that of LICs (3.36 ± 0.6) [t (7.76) = -3.37, P = 0.01] (Fig. 3C).

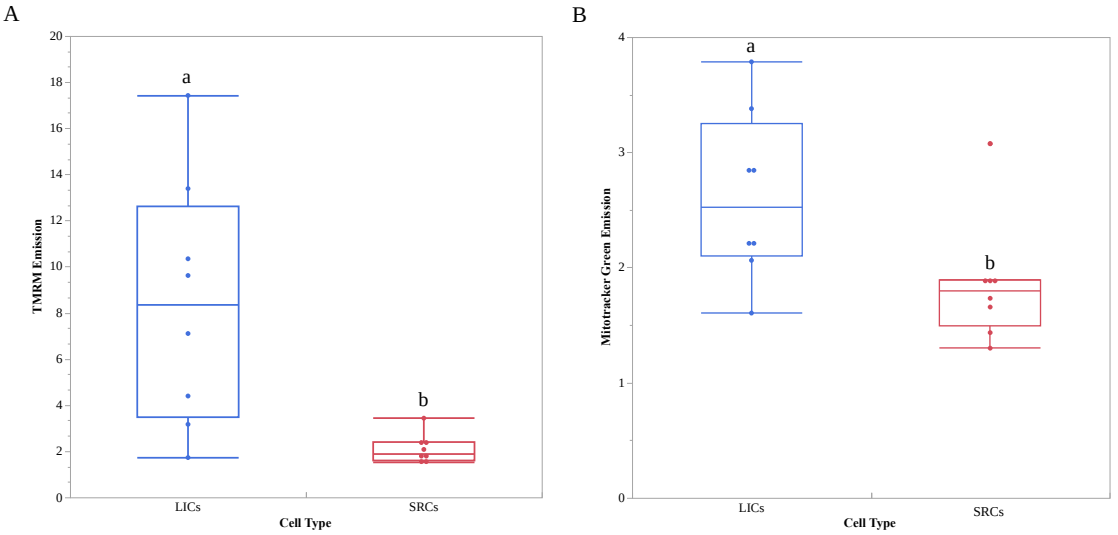

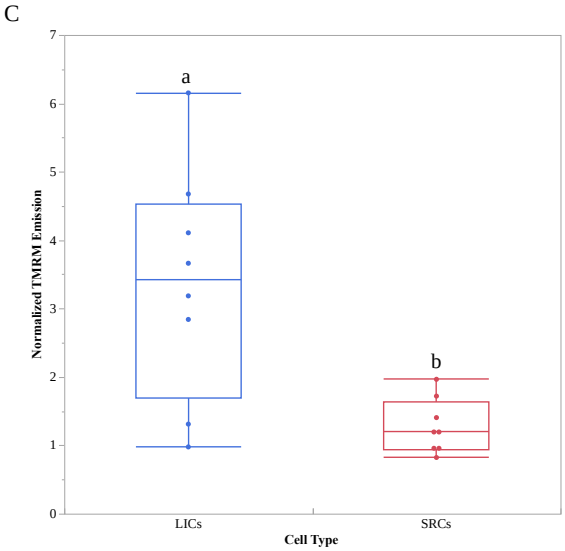

Figure 3. Mitotracker Green and TMRM fluorescence markers differ among *C. virescens* larval midgut cell populations. (A) The TMRM fluorescence intensities of LICs and SRCs. (B) The mitochondrial mass of LICs and SRCs was represented by MTG. (C) The normalized mitochondrial membrane intensities (TMRM/MTG) of LICs and SRCs. Different letters over bars signify values significantly differ ($\alpha = 0.05$).

4. Discussion

In lepidopteran larval midgut cells, the identification of stem cells among different stages could help better elucidate gut cell origin, maintenance, and differentiation (Corley and Lavine 2006). This can in turn lead to further guidance in understanding the midgut development, physiology, and the responses to injuries or infection (Hakim et al. 2001, Castagnola et al. 2011). Historically, in lepidopteran larval midguts, cells have been distinguished based on gross morphology (Loeb and Hakim 1996, Bjerknes and Cheng 2005). In our study, we developed the method of using multiple vital fluorescence markers indicative of different physiological properties in midgut cells.

Our initial observations confirmed that there are two general morphologies of midgut cells. One is larger cells containing columnar cells with their brush-like border and goblet cells with their center pitcher structure, and these cells were more irregular in shape because of microvilli and goblet cavity. Smaller cells were also visualized, likely representing a combination of stem and endocrine cells (Endo and Nishiitsutsuji-Uwo 1981). Both are more circular and regular in shape because stem cells are in an undifferentiated state, while endocrine cells are limited by the distinct membrane developed from Golgi (Endo and Nishiitsutsuji-Uwo 1981). Although morphology allowed broad separation of cells that typically localize to the apical versus basal aspect

of the gut epithelium (ie, columnar + goblet from stem + endocrine), and generally separation of columnar cells from goblet cells, we were unable to distinguish stem from endocrine based on morphology. Therefore, we examined the potential of vital dyes to assist in this.

We first tested the ability of calcein AM and TMRM staining in discriminating midgut cell subpopulations. Calcein AM intensity is proportional to cellular general esterase activity. Calcein AM staining previously was found to be elevated in small midgut cells in both *C. virescens* and *Chilo suppressalis* (Castagnola et al. 2011, Zhou et al. 2019). Calcein AM staining is also suggested to have the potential for CSCs identification (Allen et al. 2009, Chu and Sam 2019). Therefore, we hypothesized that stem cells, a subpopulation of the SRCs, would exhibit elevated calcein AM values. However, we did not find a significant difference in calcein AM fluorescence in LICs and SRCs populations. Sample isolation and analysis may account for this: Castagnola et al. (2011) and Zhou et al. (2019) separated the midgut cells through a density gradient yielding enriched small and large cell populations, while we examined a crude population, and both other groups analyzed cells by flow cytometry, a more sensitive approach less prone to photobleaching than the fluorescence microscopy used here (Muratori et al. 2008). An integrated analysis, comparing the discrimination ability and reliability of flow cytometry relative to fluorescence microscopy, for lepidopteran midgut cells is therefore needed to determine the utility of calcein AM for identifying midgut stem cells.

TMRM was used to examine differences in mitochondrial membrane potential ($\Delta\Psi_m$) between LICs and SRCs in *C. virescens* midgut cells. The $\Delta\Psi_m$ value reflects the functional condition of the mitochondria by association with the catabolic substrate in energy production (e.g., primarily glycolytic or oxidative) as well as death signal integration (Ye et al. 2011). Our results showed that LICs had much higher $\Delta\Psi_m$ than SRCs. $\Delta\Psi_m$ has been suggested to influence the stem cell state and therefore might indicate the utility of $\Delta\Psi_m$ in midgut stem cell identification (Savignan et al. 2004). When differentiation of human calcium- and temperature-dependent keratinocyte cells was induced, the $\Delta\Psi_m$ of cells decreased (Savignan et al. 2004). Reducing $\Delta\Psi_m$ enhanced HSCs function (Mantel et al. 2010). Given that stem cells are the only multiplicative and differentiable cells in the midgut, they may exhibit decreased $\Delta\Psi_m$. Unfortunately, we did not observe a discontinuous distribution of $\Delta\Psi_m$ in SRCs, which otherwise might have been indicative of multiple subpopulations of SRCs, such as stem, differentiating, and endocrine cells.

The relationship between $\Delta\Psi_m$ and differentiation in stem cells is complicated. Mouse ESCs sorted for low $\Delta\Psi_m$ ($\Delta\Psi_m$ *L*) and high $\Delta\Psi_m$ ($\Delta\Psi_m$ *H*) had indistinguishable morphology, but different metabolic rates and differentiation outcomes. $\Delta\Psi_m$ *L* cells had high mesodermal differentiation and low teratoma formation efficiency, while $\Delta\Psi_m$ *H* cells were the opposite (Schieke et al. 2008, Parker et al. 2009). The basis for this difference in stem cell fate might be due to cell replenishment or curable strategies for tissue injuries. Additionally, osteoblasts, less potent progenitor cells, exhibited higher (hyperpolarized) $\Delta\Psi_m$ than immature cells, while lung cancer stem cells (LCSCs) showed

higher $\Delta\Psi_m$ than do non-cancerous lung cells (Komarova et al. 2000, Ye et al. 2011). These last groups indicate that $\Delta\Psi_m$ reflects physiological state, which is likely more plastic than morphology. While our findings indicate the inability to identify subpopulations through morphometrics, it may be that the mitochondrial state is sufficient to distinguish cells including subpopulations. However, more study is necessary to test this, including an examination of metabolic substrate usage of midgut cells.

In addition to $\Delta\Psi_m$, we examined mitochondrial load in midgut cells, finding LICs possessed more mitochondria than SRCs. Mitochondrial mass differs within cell types, as it is tied to cell state. In stem cells, the mitochondrial load is tied to the proliferation process and ATP synthesis (Lee et al. 2002). A reduced mitochondrial number has been proposed to be related to stem cell fate. Undifferentiated ESCs and pluripotent stem cells (iPSCs) showed lower mitochondrial mass (Ye et al. 2011). Different from *C. virescens* midgut cells, lung CSCs (LCSCs) and non-lung CSCs had no difference in mitochondrial mass even though LCSCs had less mitochondrial DNA (Ye et al. 2011).

Normalizing $\Delta\Psi_m$ by mitochondrial mass yielded no change in the results: LICs exhibited higher normalized $\Delta\Psi_m$ than the SRCs. This may indicate that *C. virescens* midgut stem cells prefer glycolysis over oxidative phosphorylation. Other studies have observed this preference in stem cells for ATP production. For example, mouse HSCs utilize glycolysis instead of mitochondrial respiration (de Almeida et al. 2017).

Additionally, a metabolic shift only happened during the differentiation of mouse ESCs stem cells, from anaerobic glycolysis to mitochondrial respiration (Ravera et al. 2018).

Given our above findings, it may be useful to test the ability of a differentiation or proliferation inhibitor during midgut cell culturing to provide a binary separation of undifferentiated stem and terminally-differentiated cells. Differential activity of xenobiotic efflux pumps also may affect the observed values, as HSCs have been found to extrude MTG, reducing its accuracy in reflecting mitochondrial mass (de Almeida et al. 2017). Similarly, previous work has suggested calcein AM fluorescence may reflect a balance between esterase activity (increasing emission) and ATP-binding cassette transporter activity (decreasing emission) (Chu and Lee 2009). Consequently, concomitant clarification of gut cell physiology may provide insight into marker utility. Finally, the analyses here were of intermolt midguts. As stem cell differentiation and division patterns likely reflect molt process, studies examining marker characteristics pre-, during, and post-molt would be useful.

While the vital dyes we examined cannot conclusively distinguish stem from endocrine cells, they do open the possibility that they could be included in additional criteria in techniques such as flow cytometry to separate small round cells. Inclusion of, for example, proliferation and differentiation modifiers and markers may further allow distinction. Regardless, incorporation of mitochondrial state in identification of midgut stem cells may increase confidence in future work.

CHAPTER THREE

CHARACTERIZE THE ESCARGOT (ESG) GENE OF LEPIDOPTERAN LARVAL MIDGUT STEM CELLS

1. Abstract

Snail family members are known to be involved in stem cell maintenance and fate decisions. The snail homolog Escargot (Esg), a stemness maintainer of adult intestinal stem cells in the fly *Drosophila melanogaster*, has not been reported in other insect orders. We demonstrate here that *escargot* gene is present in lepidopteran genomes and is transcribed in the midgut of the larval noctuid *Chloridea virescens*. The possible conserved function of esg protein is also supported by the close relationship of *C. virescens* esg sequence to other lepidopteran snail homologs, as well as that of the beetle *Tribolium castaneum* and *D. melanogaster*. *C. virescens esg* transcript levels increased immediately prior to molt or pupation, but non-significantly. This suggests the role of *esg* in maintaining the stemness of stem cells may be through post-translational regulation. These findings support the hypothesis that esg is a critical stem cell factor in the lepidopteran *C. virescens* and more broadly.

2. Introduction

Identifying external cues like signaling molecules secreted from stem cell niches has greatly progressed understanding of stem cell biology. Despite this, many of the mechanisms behind the regulation of stemness remain to be identified. Knowing the specific genes, proteins, and pathways regulating the switch between self-renewal and

differentiation could aid in stem cell identification, manipulation, and clinical treatment (Barker 2014).

Numerous stem-cell expressed molecules that regulate their state have been identified in various animals. For example, in mouse, the ability of Msi1 protein in maintaining the capacity for self-renewal suggested its potential as a neural stem cell marker (Sakakibara et al. 1996). In addition to Msi, *leucine-rich-repeat-containing G-protein-coupled receptor 5 (Lgr5)* marks mouse crypt base columnar (CBC) stem cells, because the expression of *Lgr5* was restricted at the base of adult intestinal crypts (Barker et al. 2007).

The Snail-related zinc-finger transcription factor family has been implicated in stem cell maintenance in the model insect, the fly *D. melanogaster* (Korzelius et al. 2014). There are three Snail family members in *D. melanogaster*: *Escargot* (*esg*), *snail*, and *worniu*. After the initial cloning of *snail* in *D. melanogaster*, additional *snail*-orthlogues have been isolated in other species like *Tribolium castaneum* (beetle), *Achaearanea tepidariorum* (spider), the frog *Xenopus laevis*, chicken, and mouse (Kerner et al. 2009). Besides *D. melanogaster snail*, five paralogs of *snail* have been identified in *D. melanogaster* and two of them have high sequence similarity with *esg*, *snail*, and *worniu* (Kerner et al. 2009). The Snail family is part of the larger Snail superfamily, which comprises Snail and Scratch families (Manzanares et al. 2001). The Snail family members *snail*, *esg* and *worniu* are involved in forming variable structures in *D. melanogaster* by functioning in several cellular process like cell behavior, cell shape, cell

asymmetric divisions, cell fate regulation and cell differentiation (Kerner et al. 2009), while *D. melanogaster scratch* mainly promotes neural cell fate (Roark et al. 1995).

In the *D. melanogaster* adult gut, only ISCs and their daughter enteroblasts highly express *esg*; their fates are determined by *esg* (Korzelius et al. 2014). The loss of *esg* induces progenitor cells (ISCs and enteroblasts) to differentiate into enterocytes (EC) or entero-endocrine cells (EE) rapidly, while the overexpression of *esg* maintains the ISCs in the stem cell stage (Korzelius et al. 2014, Loza-Coll et al. 2016). Esg act through the Notch signaling pathway to repress differentiation-related genes in the *Drosophila* gut (Korzelius et al. 2014). In mammals, the overexpression of Snail induces the epithelial to mesenchymal transition, and the inhibition of its paralog Slug blocks the maintenance of mammary stem cell activity (Cano et al. 2000, Guo et al. 2021). When *D. melanogaster* testis cyst stem cells expressed a mutant form of *esg*, they lost the ability in maintaining as stem cells but still could proliferate (Loza-Coll et al. 2016). In summary, Snail family members are known to be pivotal in regulating stem cell fate in multiple, phylogenetically diverse systems. However, the breadth of phylogenetic conservation, as well as many of the detailed mechanisms by which the members affect stem cell physiology, remains to be explored.

To date, no *esg* homolog has been reported in the most diverse animal group on earth, the insects, other than that of *D. melanogaster*. So, this study aimed to first identify the presence of *esg* orthologue in the genome of the lepidopteran *C. virescens* through public database analysis, followed by isolation of *Cv-esg* transcript. Following that, expression levels of *esg* during different development stages of larval were analyzed. The

data obtained from this work provides the ability to test the potential of esg to serve as a marker for lepidopteran midgut stem cell identity and physiological dynamics, as well as perform tests of its function in midgut physiology.

3. Materials and Methods

3.1 Insects

C. virescens larvae were obtained from Benzon Research (Carlisle, PA) and maintained at room temperature on the diet they were shipped with. Head capsule slippage was used to signal larvae molting and new stage development (Capinera 2012). Third and 4th instar duration were each three days, while 5^{th} instar duration was six to seven days. Larvae were collected in subsequent analyses from 10 development periods: 2^{nd} instar; early, mid and late of 3^{rd} (day 1, 2, 3), 4^{th} (day 1, 2, 3) and 5^{th} (day 1-2, 3-4, 5-6) instar.

3.2 Midgut dissection and midgut cell isolation

Before dissection, work surfaces, pipettes, and dissection materials were decontaminated with RNase Away (Molecular BioProducts). To isolate midguts for subsequent analysis, *C. virescens* larvae were anesthetized on ice for 5mins. The surface of the larvae was sterilized by brief immersion in a sterile washing solution (3% Dawn liquid dish detergent + 30% sterile distilled-deionized water + 67 % Clorox bleach). Midgut dissection was immediately performed after transferring the larva onto a wax dissection plate containing sterile Ringer's solution (137 mM NaCl, 1.8 mM $CaCl_2$, 2.7 mM KCl, 2.4 mM $NaHCO_3$) (Castagnola et al. 2011). The larval head and telson were

immobilized with sterile dissection pins, then the entire dorsal midline was cut from the posterior to the anterior to expose the gut. Gut contents, peritrophic membrane, and the Malpighian tubules were cleaned from the larval midgut by sterile dissection scissors. The excised midgut was rinsed briefly in 3mL sterile Ringer's solution, then transferred to 1.7mL RNase-free microtubes.

Four larval midguts from each developmental stage were collected for developmental expression analysis. The collection was repeated three times. Four whole larvae from 10 different development stages were also collected. Whole larva samples were used for *esg* cloning.

3.3 RNA isolation and cDNA synthesis

Midguts or whole larvae were homogenized in cold (4°C) TRIzol™ Reagent (Invitrogen) with sterile homogenizers. 1mL TRIzol Reagent was added per 50–100 mg of wet tissue. After 5 minutes incubation, chloroform (0.2 mL per 1 mL of used TRIzol Reagent) was mixed with samples through 15s vortex. The samples were incubated for 3 minutes at room temperature, then centrifuged at 12,000 g for 15 minutes at 4°C. The colorless supernatants were transferred into new tubes. The remainder of RNA extraction followed the manufacturer's protocol. The RNA quality and concentration of samples were determined by NanoDrop (Thermo Scientific). Samples with A_{260}/A_{280} ratios ~ 2 were selected for use and stored at -80°C for cDNA synthesis.

Total RNA (3.5 μg) was reverse transcribed into cDNA using the UltraScript 2.0 Reverse Transcriptase kit (PCR Biosystems Ltd.) following the manual. For *escargot*

gene cloning, 5µl each of 2nd, 3rd, 4th, and 5th instar whole larva RNA were mixed and used in cDNA synthesis.

3.4 Cloning and sequencing of escargot and tubulin genes

The presumptive *escargot* orthologue from *C. virescens* (Genbank# NWSH01000172.1, date of access: 30- JAN-2020) was identified in public databases by sequence similarity to *D. melanogaster* (Sequence# NM_057252.4, date of access: 30-JAN-2020). The primer sets were designed using Primer3 (http://bioinfo.ut.ee/primer3-0.4.0/) based on the *C. virescens* esg DNA (Genbank# NWSH01000172.1) and putative protein coding (Genbank PCG78775.1) sequences and the reference gene *C. virescens alpha-tubulin* sequence (FJ550360.1). Primers were designed based on the following criteria: primer size lengths 18 - 22 bp, annealing temperature 55°C - 60°C, GC content between 40 and 60%, and the PCR amplification product size between 200 and1000bp. Primer sequences are listed in Table 2.

PCR amplification of *Cv-esg* for cloning was performed in a thermal cycler (VeritiPro™) with 2µL first-strand cDNA (50 µL reaction) using Phusion High-Fidelity PCR Kit (Thermo Scientific). After an initial 30 second denaturation at 98°C, 30 amplification cycles were performed as follows: 10 sec denaturation at 98°C, 30 sec annealing at 60°C, and 30 sec extension at 72°C, and then a final 10 min extension at 72°C. Tubulin PCR amplification was performed with 2µL first-strand cDNA (50µL reaction) using DreamTaq Green PCR Master Mix (Thermo Scientific). After an initial 30 sec denaturation at 95°C, 30 amplification cycles were performed as follows: 30 sec denaturation at 95°C, 30 sec annealing at 60°C, and 1 min extension at 72°C, and then a

final 10 min extension at 72°C. PCR products were purified using QIAquick PCR Purification Kit (Qiagen). Products and 5kbp DNA molecular weight ladder (Thermo Scientific) were loaded onto Ethidium Bromide stained 1% agarose gels to confirm the expected size.

Purified *esg* and *tubulin* amplification were ligated and cloned in pMiniT^{TM} 2.0 vector (NEB) and pGEM-T easy vector (Promega) separately and denoted as pMiniT/esg and pGEM/Tubulin, respectively. QIAprep Spin Miniprep Kit (Qiagen) was used to purify cloned plasmids. The size of pMiniT/esg and pGEM/Tubulin were checked by restriction digest pattern and sequencing (Eton Bioscience, Inc.).

3.5 Quantitative real-time PCR

qPCR primer sets for RT-qPCR were designed in Primer3 (version 4.1.0) based on sequencing results, with the following constraints: primer size lengths 18 - 22bp, annealing temperature 57°C - 63°C, GC content between 30 and 70%, and the PCR amplification product size between 75 and 200bp. qPCR primer sequences are listed in Table 2.

Real-time qPCR amplifications were run on CFX Connect Real-Time PCR Detection System (Bio-Rad). For each real-time qPCR mixture, 10µl 2X iQ^{TM} SYBR Green Supermix (Bio-Rad), 0.6µl of each primer (300nM) from 10µM working solution, and 1µl of cDNA sample were added and supplemented with nuclease-free water to a final 20µl reaction volume. The thermal cycling program consisted of 3 min initial denaturation at 95°C, 40 cycles of 10 sec denaturation at 95°C, 20 sec annealing at 60°C, and 30 sec extension at 72°C. The fluorescent signals were monitored at the end of each

cycle. After the amplification reactions were completed, the melting curve analysis routinely was performed (55°C to 95°C in 0.5°C increments for 5 sec each). Three biological replicates of each development stage were performed. Each sample had three technical replicates using *esg* and *Tubulin* gene qPCR primers. Each reaction plate contained a standard curve of pMiniT*/esg* to check the efficiency of the reaction and no-template controls.

Before measuring the expression level of each cDNA sample, six 10-fold serial dilution series of *pMiniT/esg* and *pGEM/Tubulin* ranging from 25ng/µl to 0.00025ng/µl were used in standard curve construction, to check primer efficiency.

3.6 Data analysis

Real-time qPCR data were collected with CFX Maestro software (version 2.2, Bio-rad) and exported into Microsoft Excel for initial analysis. Standard curves were generated using relative concentration and the C_T value, which is the number of cycles when the fluorescent signal of the sample exceeded the specific threshold of detection and is inversely proportional to the quantity of templates in the reaction (McCurley and Gloria 2008). The slope of the standard curve was applied in the calculation of PCR amplification efficiency (E) based on the equation: $\%E = (-1 + 10^{[-1/slope]}) \times 100\%$. The correlation coefficient (R^2) was also generated.

The average C_T values of three technical replicates were calculated in Microsoft Excel first. The *esg* fold gene expression values were calculated with the $2^{-\Delta\Delta CT}$ method where,

$\Delta CT = (C_T$ of the target gene - C_T of the reference gene),

ΔΔCT: ΔC_T of the sample - ΔC_T of the calibrator (Pfaffl 2002).

The ΔCT value of the first day of the third stage was used as a calibrator. The values obtained by this relative quantification method were tested for normality of distribution and homoscedasticity, then analyzed by Kruskal-Wallis ranked sum test in R Studio (PBC, Boston, MA, USA). P-values < 0.05 were set as significant. Figures were made by JMP software (version 16.0, SAS Institute, Cary, NC, USA).

Sequence alignments were performed with CLUSTALW (https://www.genome.jp/tools-bin/clustalw) and figures were made by ESPript 3.0 (https://espript.ibcp.fr/ESPript/cgi-bin/ESPript.cgi) (Robert and Gouet 2014).

Table 2. Sequences of primers for PCR and real-time qPCR. (F: Forward Primers, R: Reverse Primers)

Gene	Accession no.	Primer sequence (5′ → 3′)	Length (nt)	Product size (bp)
Esg (PCR)	PCG78775.1	F：GAAAATGACGAACCCCAAAA	20	624
		R: ACATTTACAGGGCAGGGTGT	20	
Esg (qPCR)	PCG78775.1	F: CCACCTTCCTCTGTGTCACC	20	123
		R: ACAATCTGGGCACTGGTAGC	20	
Tubulin (PCR)	FJ550360.1	F: AGATGCCCACAGACAAGACC	20	587
		R: GAGACGGTTCAGGTTGGTGT	20	
Tublin (qPCR)	FJ550360.1	F: CAACAACTATGCCCGTGGAC	20	162
		R: ATGAGGAGGGAGGTGAAACC	20	

4. Results

4.1 Isolation and cloning of C. virescens esg *orthologue*

Based on the sequence of *D. melanogaster esg* (Genbank# NT_033779.5), a putative *C. virescens* (Genbank# NWSH01000172.1) *esg* orthologue was identified (Fig 1A). A partial *C. virescens escargot* (*Cv_esg*) sequence was amplified (Fig. 1B) from whole-body larval cDNA using primers designed based on *C. virescens* B5V51_3066, then cloned into pMinit 2.0 vector and sequenced. The cloned nucleotide sequence of *Cv-esg* was 624bp. The pairwise comparison of the B5V51_3066 (HvSNL1) coding sequence with *pMinit/esg* sequencing result (*Cv-esg*) indicated a cloned *esg* homologue expressed in larval *C. virescens* with two mismatches (Fig. 1C). Alignment of the translated cloned product with PCG78775.1 (HvSNL1) shows that the two nucleotide mismatches are predicted to be conservative, resulting in the same amino acid sequence (Fig. 1D).

The translated *Cv*-esg protein sequence was further aligned with multiple predicted snail-like protein sequences of the Lepidoptera *Trichoplusia ni* (cabbage looper), *Helicoverpa zea* (corn earworm), *Helicoverpa armigera* (corn earworm), and *Spodoptera frugiperda* (all members of family Noctuidae), and *Plutella xylostella* (diamondback moth) and *Bombyx mori* (domestic silk moth), as well as the fly *D. melanogaster* and beetle *Tribolium castaneum* (Fig. 1D). The snail-like protein sequences are highly similar among Lepidoptera species (Fig. 1D). For insects from different orders, they had high similarity in carboxyl-terminal (C) end of esg protein sequences (Fig. 1D).

4.2 Esg expression patterns during C. virescens *development*

Starting from the first day of 3rd instar, midguts were collected for total RNA isolation. *C. virescens* larvae exhibited 5 instars in total, stereotypically spending 3 days in the 3rd instar, 3 days in the 4th instar, and 7-8 days in the 5th instar. We denoted periods during instar as early (d1), mid (d2), and late (d3) for the 3rd or 4th instar. For the 5th instar, the 1st and 2nd days, the 3rd and 4th days, the 5th and 6th days, and the 7th and 8th days were considered as early, mid, late, and pupa phases, respectively (Tettamanti et al. 2017).

The mid-phase of both the 3rd and 4th instar showed the lowest *esg* expression level, but the mid-phase of the 5th instar did not (Fig. 2). The *esg* expression level was the highest at the late phase of the 3rd, 4th, and 5th instar then dropped again at the beginning of the new phase (Fig. 2). Noticeably, before entering the pupal phase, the expression level of *esg* in the late 5th instar showed the highest amount compared to all phases (Fig. 2). *Esg* transcript levels did not statistically differ among developmental stages (Fig. 2) ($P = 0.1695$).


A
GM04789p [Drosophila melanogaster]
Protein escargot [Eumeta japonica]
protein snail homolog Sna [Plutella xylostella]
zinc finger protein SNAI2 [Manduca sexta]
butterflies | 4 leaves
butterflies | 2 leaves
butterflies | 2 leaves
zinc finger protein SNAI2-like [Maniola hyperantus]
zinc finger protein SNAI2-like [Zerene cesonia]
zinc finger protein SNAI2-like [Pieris rapae]
unnamed protein product [Pieris macdunnoughi]
zinc finger protein SNAI2-like [Aricia agestis]
moths | 2 leaves
zinc finger protein SNAI2-like [Hyposmocoma kahamanoa]
zinc finger protein SNAI2-like [Galleria mellonella]
moths | 2 leaves
zinc finger protein SNAI2-like [Ostrinia furnacalis]
unnamed protein product [Arctia plantaginis]
unnamed protein product [Arctia plantaginis]
zinc finger protein SNAI2-like [Trichoplusia ni]
hypothetical protein B5V51_3066 [Heliothis virescens]
moths | 2 leaves
zinc finger protein SNAI2-like [Spodoptera litura]
hypothetical protein HW555_007454 [Spodoptera exigua]
zinc finger protein SNAI2-like [Spodoptera frugiperda]
0.1

B

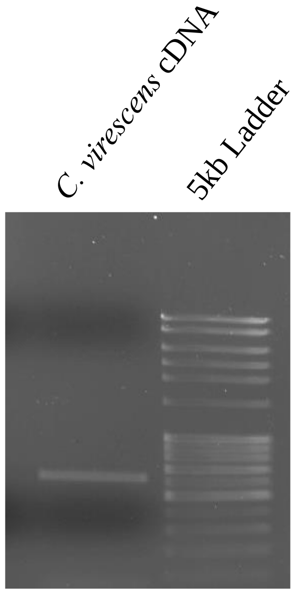
C. virescens cDNA
5kb Ladder

C

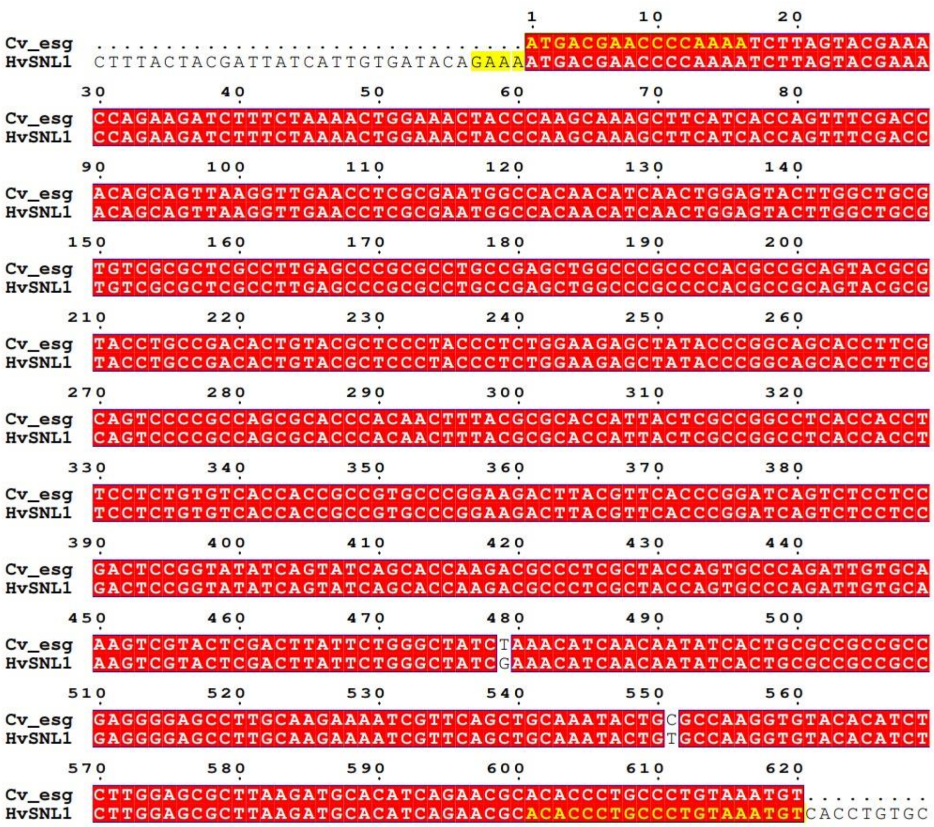
1 10 20
Cv_esg ..............................ATGACGAACCCCAAAATCTTAGTACGAAA
HvSNL1 CTTTACTACGATTATCATTGTGATACAGAAAATGACGAACCCCAAAATCTTAGTACGAAA
30 40 50 60 70 80
Cv_esg CCAGAAGATCTTTCTAAAACTGGAAACTACCCAAGCAAAGCTTCATCACCAGTTTCGACC
HvSNL1 CCAGAAGATCTTTCTAAAACTGGAAACTACCCAAGCAAAGCTTCATCACCAGTTTCGACC
90 100 110 120 130 140
Cv_esg ACAGCAGTTAAGGTTGAACCTCGCGAATGGCCACAACATCAACTGGAGTACTTGGCTGCG
HvSNL1 ACAGCAGTTAAGGTTGAACCTCGCGAATGGCCACAACATCAACTGGAGTACTTGGCTGCG
150 160 170 180 190 200
Cv_esg TGTCGCGCTCGCCTTGAGCCCGCGCCTGCCGAGCTGGCCCGCCCCACGCCGCAGTACGCG
HvSNL1 TGTCGCGCTCGCCTTGAGCCCGCGCCTGCCGAGCTGGCCCGCCCCACGCCGCAGTACGCG
210 220 230 240 250 260
Cv_esg TACCTGCCGACACTGTACGCTCCCTACCCTCTGGAAGAGCTATACCCGGCAGCACCTTCG
HvSNL1 TACCTGCCGACACTGTACGCTCCCTACCCTCTGGAAGAGCTATACCCGGCAGCACCTTCG
270 280 290 300 310 320
Cv_esg CAGTCCCCGCCAGCGCACCCACAACTTTACGCGCACCATTACTCGCCGGCCTCACCACCT
HvSNL1 CAGTCCCCGCCAGCGCACCCACAACTTTACGCGCACCATTACTCGCCGGCCTCACCACCT
330 340 350 360 370 380
Cv_esg TCCTCTGTGTCACCACCGCCGTGCCCGGAAGACTTACGTTCACCCGGATCAGTCTCCTCC
HvSNL1 TCCTCTGTGTCACCACCGCCGTGCCCGGAAGACTTACGTTCACCCGGATCAGTCTCCTCC
390 400 410 420 430 440
Cv_esg GACTCCGGTATATCAGTATCAGCACCAAGACGCCCTCGCTACCAGTGCCCAGATTGTGCA
HvSNL1 GACTCCGGTATATCAGTATCAGCACCAAGACGCCCTCGCTACCAGTGCCCAGATTGTGCA
450 460 470 480 490 500
Cv_esg AAGTCGTACTCGACTTATTCTGGGCTATCTAAACATCAACAATATCACTGCGCCGCCGCC
HvSNL1 AAGTCGTACTCGACTTATTCTGGGCTATCGAAACATCAACAATATCACTGCGCCGCCGCC
510 520 530 540 550 560
Cv_esg GAGGGGAGCCTTGCAAGAAAATCGTTCAGCTGCAAATACTGCGCCAAGGTGTACACATCT
HvSNL1 GAGGGGAGCCTTGCAAGAAAATCGTTCAGCTGCAAATACTGTGCCAAGGTGTACACATCT
570 580 590 600 610 620
Cv_esg CTTGGAGCGCTTAAGATGCACATCAGAACGCACACCCTGCCCTGTAAATGT.........
HvSNL1 CTTGGAGCGCTTAAGATGCACATCAGAACGCACACCCTGCCCTGTAAATGTCACCTGTGC

D

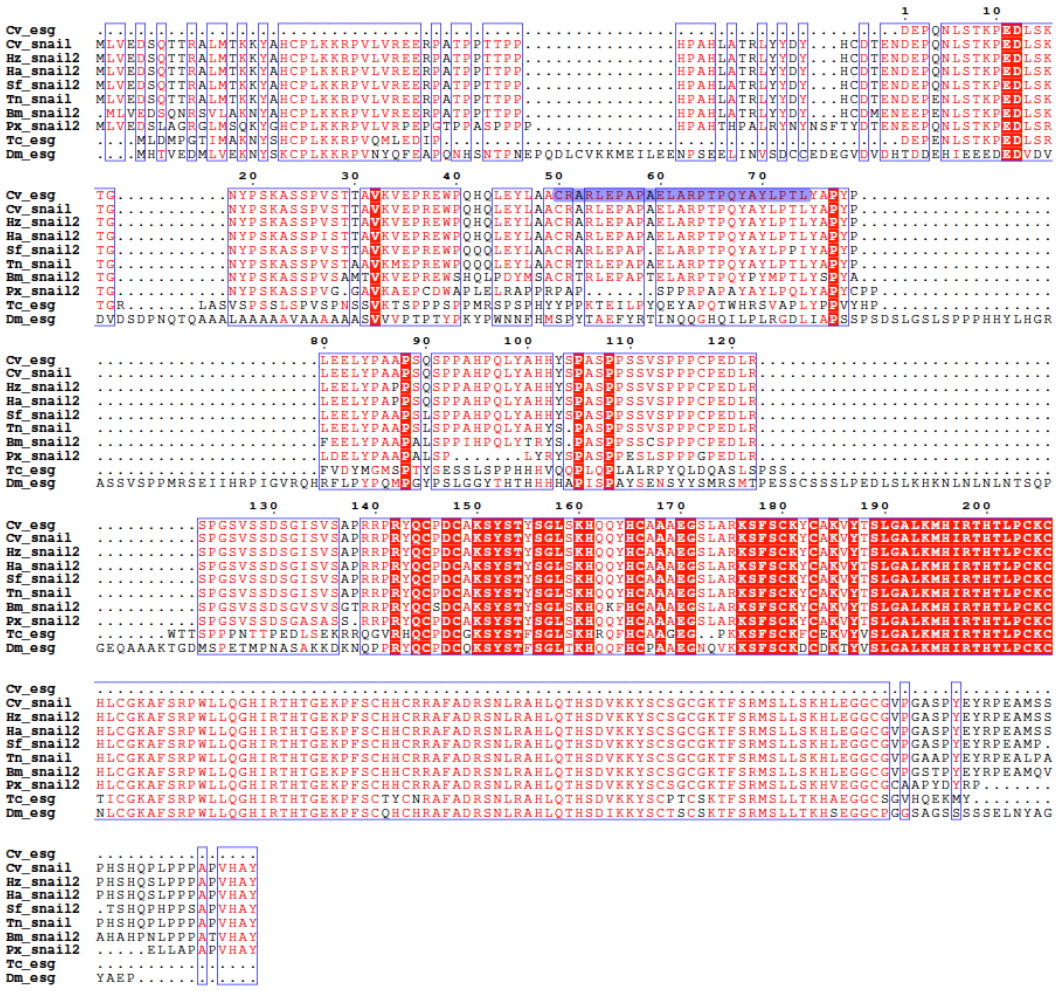

Figure 4. Cloning of *C. virescens escargot* homologue. (A) Phylogenetic tree of *D. melanogaster esg* sequence, a putative *C. virescens* homolog, and another lepidopteran snail homolog. (B) A partial *C. virescens esg* (*Cv-esg*) sequence was present (box) in the whole-body larval cDNA. (C) Sequence alignment of B5V51_3066 (HvSNL1) coding sequence and *Cv-esg*. Identical nucleotides among sequences were colored red. Primers were marked with yellow. (D) Multiple alignments of predicted snail-like protein and esg of insects. Amino acids marked with purple are peptide sequences of esg antibody.
Cv_esg: Translated protein sequence based on *pMinit/esg* sequencing.
Cv_snail: *Chloridea virescens* hypothetical protein B5V51_3066
Hz_snail2: *Helicoverpa zea* predicted zinc finger protein SNAI2-like (LOC124645725).
Ha_snail2: *Helicoverpa armigera* predicted zinc finger protein SNAI2-like (LOC110375494)
Sf_ snail2: *Spodoptera frugiperda* predicted zinc finger protein SNAI2-like (LOC118273623)

Tn_ snail: *Trichoplusia ni* predicted zinc finger protein SNAI2-like (LOC113501420)
Bm_ snail2: *Bombyx mori* predicted zinc finger protein SNAI2 (LOC101744234)
Px_ snial2: *Plutella xylostella* predicted protein snail homolog Sna (LOC105387329)
Tc_esg: *Tribolium castaneum* escargot
Dm_esg: *Drosophila melanogaster* escargot

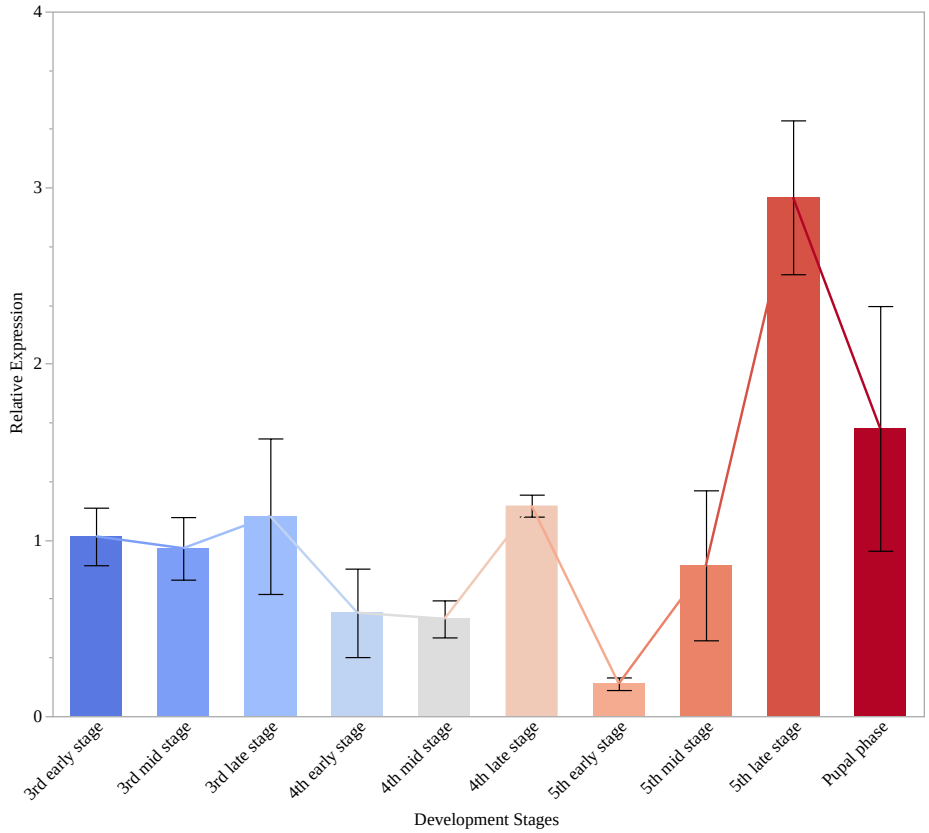

Figure 5. Expression analysis of *esg* transcripts in *C. virescens* larvae during different developmental instars. The relative expression levels of *esg* were normalized by the expression of reference gene *C. virescens tubulin*. Each error bar was constructed using the standard error of the mean.

5. Discussion

In this study, the *C. virescens* orthologue of the *D. melanogaster escargot* gene of the Snail gene family was identified and cloned. Blast analysis with *Cv-esg* identified numerous similar coding sequences across lepidopteran databases (Fig. 1A), supporting

conservation of *esg* in Lepidoptera. Multiple alignment showed the close relationship of *Cv-esg* with other lepidopteran snail homologs, as well as with those of the model beetle, *T. castaneum,* and *D. melanogaster* (Fig. 1D) suggesting possible functional conservation. Strong protein conservation also suggests potential for immune reagents to be broadly applicable.

Although the function of *Cv-esg* was not tested in this study, the pattern of transcripts (Fig. 2) suggests testable hypotheses. Throughout *D. melanogaster* embryo development, *esg* exhibits a dynamic expression pattern and is mainly expressed in ectodermal layers (Whiteley 1992). Null *Dm-esg* mutants are embryonic lethal, while global loss in larvae also is lethal suggesting the *esg* product is important for continued development (Whiteley 1992). However, intestinal *esg* transcript patterns in *D. melanogaster* larvae are lacking. *Cv-esg* transcripts are present in midgut tissue throughout 2^{nd} – 5^{th} instars. *Cv-esg* levels appear to increase in late stages relative to early- and mid-stages of each instar. This suggests that *esg* may play a role in maintaining the stemness of stem cells during intermolt stages (early- and mid-stage) prior to an increased expression immediately prior to molt or pupation. However, transcript level differences were not statistically significant. This could be due to post-translational regulation of *Cv-esg* in the larval midgut, requiring utilization of an anti-*Cv*-esg antibody. At this time, there are no insect-specific escargot antibodies available.

Given observations and experiments in *D. melanogaster*, I hypothesize that *Cv*-esg functions to maintain the stemness of midgut stem cells. Future work to investigate *Cv-esg* function will utilize antibodies to examine protein levels and localization, as well

as analysis of cultured stem cells during phases of activity including quiescence and differentiation. Given protein similarities, this work potentially could extend to the global pests *Helicoverpa armigera*, *H. zea*, *Plutella xylostella,* and *Spodoptera frugiperda*, as well.

CHAPTER FOUR

CONCLUSION

The midgut of the larval stage of lepidopteran is a complex structure that plays a role in the digestive system and absorptive system in the insects (Hakim et al. 2001). There are four types of cells in lepidoptera larval midgut which are categorized into mature cells (columnar, goblet and endocrine cells) and stem cells. Mature cells function in digestive enzymes production, small organic nutrients, ions transportation important signals production (Caccia et al. 2019). Stem cells are responsible for the self-renewal and mature cell replenishment during the development of the midgut. The proliferation and differentiation of stem cell help maintain the stability of midgut and repair the injured midgut (Castagnola et al. 2011). Several experiments have suggested that stem cells play a critical role in recovering from Bt Cry toxin, which is a commonly used insecticide targeting the midgut epithelium (Tabashnik 1994, Bretschneider et al. 2016). Better understanding of stem cells function in the lepidopteran midgut could give more guidance of controlling the resistance toward Bt (Tabashnik 1994, Heckel et al. 2007, Tabashnik et al. 2013). However, the lack of specific and reliable markers for lepidopteran midgut stem cells hinders this progress.

In our first study, we developed two vital fluorescence markers (TMRM and MTG) that indicate $\Delta\Psi_m$ and mitochondrial mass, respectively, in midgut cell discrimination. During testing, we also examined another commonly applied vital marker, Calcein AM, which represents the esterase activity of cells. From initial observation on general morphologies, there are two distinguishable populations of cells.

Larger cells are a mix of columnar and goblet cells, which both are more irregular in shape (here termed LICs), while smaller cells are likely a mix of stem and endocrine cells, which both are round and more regular in shape (here termed SRCs) (Endo and Nishiitsutsuji-Uwo 1981). Surprisingly, our analyses of calcein AM intensity was incapable of separating these two cell groups, given previous studies showed calcein AM intensity differs in human CSCs and non-CSCs, and midgut stem and mature cells of the larval lepidopterans *C. suppressalis* and *C. virescens* (Allen et al. 2009, Castagnola et al. 2011, Zhou et al. 2019). We postulate that the inconsistency may be due to differences in cell separation (e.g., duration of dye incubation) or analysis (i.e., microscopy rather than flow cytometry) methodology.

Unlike with calcein AM staining, LICs and SRCs differed from each other in both $\Delta\Psi_m$ and mitochondrial mass. LICs are higher in $\Delta\Psi_m$, indicating hyperpolarization of the mitochondrial membrane, and possess more mitochondrial than SRCs; together, these data suggest greater (potential for) rates of oxidative phosphorylation of LICs than SRCs. Frustratingly, there was no apparent discontinuity in $\Delta\Psi_m$, mitochondrial mass, or Normalized $\Delta\Psi_m$ in the SRC pool. This lack frustratingly prevents separation of presumptive endocrine and stem cells within the SRC pool. Further studies are needed to overcome this ability, perhaps by triple vital dye staining with flow cytometry, along with use of inhibitors of proliferation and differentiation.

Our second study investigated *C. virescens* midgut stem cells by identifying a stemness maintainer gene, *escargot* (*esg*) which in insects only has been examined in the fly *D. melanogaster*. We identified that esg is encoded in the genome of the lepidopteran

C. virescens and numerous other members of that order, and its sequence is highly conserved across other insect species. The *esg* gene expression level among different larval development stages implies it functions in midgut stem cell maintenance as in *D. melanogaster*, but protein-level studies are needed.

In conclusion, these combined studies provide reference for future research into isolation and characterization of lepidopteran larval midgut stem cells and their energetics, as well as the stem cell fate relevant gene esg. These data also have potential application for modifying stem cell activity and developing esg antibody.

REFERENCES

Allen, J.E., Hart, L.S., Dicker, D.T., Wang, W. and El-Deiry, W.S., 2009. Visualization and enrichment of live putative cancer stem cell populations following p53 inactivation or Bax deletion using non-toxic fluorescent dyes. *Cancer biology & therapy*, 8(22), pp.2193-2204.

Apidianakis, Y. and Rahme, L.G., 2011. *Drosophila melanogaster* as a model for human intestinal infection and pathology. *Disease models & mechanisms*, 4(1), pp.21-30.

Barker, N., 2014. Adult intestinal stem cells: critical drivers of epithelial homeostasis and regeneration. *Nature reviews Molecular cell biology*, 15(1), pp.19-33.

Barker, N., Van Es, J.H., Kuipers, J., Kujala, P., Van Den Born, M., Cozijnsen, M., Haegebarth, A., Korving, J., Begthel, H., Peters, P.J. and Clevers, H., 2007. Identification of stem cells in small intestine and colon by marker gene Lgr5. *Nature*, 449(7165), pp.1003-1007.

Bilbo, T.R., Reay-Jones, F.P., Reisig, D.D. and Greene, J.K., 2019. Susceptibility of corn earworm (Lepidoptera: Noctuidae) to Cry1A. 105 and Cry2Ab2 in North and South Carolina. *Journal of economic entomology*, 112(4), pp.1845-1857.

Bjerknes, M. and Cheng, H., 2005. Gastrointestinal stem cells. II. Intestinal stem cells. *American Journal of Physiology-Gastrointestinal and Liver Physiology*, 289(3), pp. G381-G387.

Blau, H.M., Brazelton, T.R. and Weimann, J.M., 2001. The evolving concept of a stem cell: entity or function? *Cell*, 105(7), pp.829-841.

Booth, C. and Potten, C.S., 2000. Gut instincts: thoughts on intestinal epithelial stem cells. *The Journal of clinical investigation*, 105(11), pp.1493-1499.

Bravo, A., Gill, S.S. and Soberon, M., 2007. Mode of action of *Bacillus thuringiensis* Cry and Cyt toxins and their potential for insect control. *Toxicon*, 49(4), pp.423-435.

Bretschneider, A., Heckel, D.G. and Pauchet, Y., 2016. Three toxins, two receptors, one mechanism: Mode of action of Cry1A toxins from Bacillus thuringiensis in *Heliothis virescens*. *Insect biochemistry and molecular biology*, 76, pp.109-117.

Caccia, S., Casartelli, M. and Tettamanti, G., 2019. The amazing complexity of insect midgut cells: types, peculiarities, and functions. *Cell and Tissue research*, 377(3), pp.505-525.

Cano, A., Pérez-Moreno, M.A., Rodrigo, I., Locascio, A., Blanco, M.J., del Barrio, M.G., Portillo, F. and Nieto, M.A., 2000. The transcription factor snail controls epithelial–

mesenchymal transitions by repressing E-cadherin expression. *Nature cell biology*, 2(2), pp.76-83.

Capinera, J.L., 2012. Tobacco Budworm, *Heliothis virescens* (Fabricius) (Insecta: Lepidoptera: Noctuidae). *EDIS*, 2012(10).

Castagnola, A. and Jurat-Fuentes, J.L., 2016. Intestinal regeneration as an insect resistance mechanism to entomopathogenic bacteria. *Current opinion in insect science*, 15, pp.104-110.

Castagnola, A., Eda, S. and Jurat-Fuentes, J.L., 2011. Monitoring stem cell proliferation and differentiation in primary midgut cell cultures from *Heliothis virescens* larvae using flow cytometry. *Differentiation*, 81(3), pp.192-198.

Chambers, I. and Smith, A., 2004. Self-renewal of teratocarcinoma and embryonic stem cells. *Oncogene*, 23(43), pp.7150-7160.

Chiang, A.S., Yen, D.F. and Peng, W.K., 1986. Defense reaction of midgut epithelial cells in the rice moth larva (*Corcyra cephalonica*) infected with *Bacillus thuringiensis*. *Journal of Invertebrate Pathology*, 47(3), pp.333-339.

Chu, K. and Lee, S.W., 2009. Revisiting calcein AM: alternative tool for identifying dye-effluxing cancer stem cells? *Cancer biology & therapy*, 8(22), pp.2205-2207.

Cioffi, M., 1979. The morphology and fine structure of the larval midgut of a moth (Manduca sexta) in relation to active ion transport. *Tissue and Cell*, 11(3), pp.467-479.

Corley, L.S. and Lavine, M.D., 2006. A review of insect stem cell types. *Seminars in cell & developmental biology*, 17(4), pp.510-517. Academic Press.

de Almeida, M.J., Luchsinger, L.L., Corrigan, D.J., Williams, L.J. and Snoeck, H.W., 2017. Dye-independent methods reveal elevated mitochondrial mass in hematopoietic stem cells. *Cell stem cell*, 21(6), pp.725-729.

Dow, J.A., 1992. pH gradients in lepidopteran midgut. *The Journal of experimental biology*, 172(1), pp.355-375.

Endo, Y. and Nishiitsutsuji-uwo, J.U.N.K.O., 1981. Gut endocrine cells in insects: the ultrastructure of the gut endocrine cells of the lepidopterous species. *Biomedical Research*, 2(3), pp.270-280.

Engel, P. and Moran, N.A., 2013. The gut microbiota of insects–diversity in structure and function. *FEMS microbiology review*s, 37(5), pp.699-735.

Fuchs, E. and Segre, J.A., 2000. Stem cells: a new lease on life. *Cell*, 100(1), pp.143-155.

Gomes, F. M., Carvalho, D. B., Machado, E. A., & Miranda, K. (2013). Ultrastructural and functional analysis of secretory goblet cells in the midgut of the lepidopteran *Anticarsia gemmatalis*. *Cell and tissue research*, 352(2), 313-326.

Guo, W., Keckesova, Z., Donaher, J.L., Shibue, T., Tischler, V., Reinhardt, F., Itzkovitz, S., Noske, A., Zürrer-Härdi, U., Bell, G. and Tam, W.L., 2012. Slug and Sox9 cooperatively determine the mammary stem cell state. *Cell*, 148(5), pp.1015-1028.

Hakim, R.S., Baldwin, K.M. and Loeb, M., 2001. The role of stem cells in midgut growth and regeneration. *In Vitro Cellular & Developmental Biology-Animal*, 37(6), pp.338-342.

Heckel, D.G., Gahan, L.J., Baxter, S.W., Zhao, J.Z., Shelton, A.M., Gould, F. and Tabashnik, B.E., 2007. The diversity of Bt resistance genes in species of Lepidoptera. *Journal of invertebrate pathology*, 95(3), pp.192-197.

Hoover, K., Washburn, J.O. and Volkman, L.E., 2000. Midgut-based resistance of *Heliothis virescens* to baculovirus infection mediated by phytochemicals in cotton. *Journal of Insect Physiology*, 46(6), pp.999-1007.

Insoft, R.M., Sanderson, I.R. and Walker, W.A., 1996. Development of immune function in the intestine and its role in neonatal diseases. *Pediatric Clinics*, 43(2), pp.551-571.

JMP®, Version <16.0>. SAS Institute Inc., Cary, NC, 1989–2021.

Kayahara, T., Sawada, M., Takaishi, S., Fukui, H., Seno, H., Fukuzawa, H., Suzuki, K., Hiai, H., Kageyama, R., Okano, H. and Chiba, T., 2003. Candidate markers for stem and early progenitor cells, Musashi-1 and Hes1, are expressed in crypt base columnar cells of mouse small intestine. *FEBS letters*, 535(1-3), pp.131-135.

Kerner, P., Hung, J., Béhague, J., Le Gouar, M., Balavoine, G. and Vervoort, M., 2009. Insights into the evolution of the snail superfamily from metazoan wide molecular phylogenies and expression data in annelids. *BMC evolutionary biology*, 9(1), pp.1-16.

Klowden, M.J., 2013. Physiological systems in insects. Academic Press.

Komarova, S.V., Ataullakhanov, F.I. and Globus, R.K., 2000. Bioenergetics and mitochondrial transmembrane potential during differentiation of cultured osteoblasts. *American Journal of Physiology-Cell Physiology*, 279(4), pp.C1220-C1229.

Korzelius, J., Naumann, S.K., Loza‐Coll, M.A., Chan, J.S., Dutta, D., Oberheim, J., Gläßer, C., Southall, T.D., Brand, A.H., Jones, D.L. and Edgar, B.A., 2014. Escargot maintains stemness and suppresses differentiation in *Drosophila* intestinal stem cells. *The EMBO journal*, 33(24), pp.2967-2982.

Lee, H.C., Yin, P.H., Chi, C.W. and Wei, Y.H., 2002. Increase in mitochondrial mass in human fibroblasts under oxidative stress and during replicative cell senescence. *Journal of biomedical science*, 9(6), pp.517-526.

Levy, S.M., Falleiros, A.M.F., Gregório, E.A., Arrebola, N.R. and Toledo, L.A., 2004. The larval midgut of Anticarsia gemmatalis (Hübner)(Lepidoptera: Noctuidae): light and electron microscopy studies of the epithelial cells. *Brazilian Journal of Biology*, 64(3B), pp.633-638.

Li, L. and Xie, T., 2005. Stem cell niche: structure and function. *Annu. Rev. Cell Dev. Biol.*, 21, pp.605-631.

Linser, P.J. and Dinglasan, R.R., 2014. Insect gut structure, function, development and target of biological toxins. *Advances in insect physiology*, 47, pp.1-37.

Liu, H., He, Z., April, S.L., Trefny, M.P., Rougier, J.S., Salemi, S., Olariu, R., Widmer, H.R. and Simon, H.U., 2019. Biochemical re-programming of human dermal stem cells to neurons by increasing mitochondrial membrane potential. *Cell Death & Differentiation*, 26(6), pp.1048-1061.

Loeb, M.J. and Hakim, R.S., 1996. Insect midgut epithelium in vitro: an insect stem cell system. *Journal of insect physiology*, 42(11-12), pp.1103-1111.

Loeb, M.J., 2010. Factors affecting proliferation and differentiation of lepidopteran midgut stem cells. *Archives of insect biochemistry and physiology*, 74(1), pp.1-16.

Loeb, M.J., Clark, E.A., Blackburn, M., Hakim, R.S., Elsen, K. and Smagghe, G., 2003. Stem cells from midguts of Lepidopteran larvae: clues to the regulation of stem cell fate. *Archives of Insect Biochemistry and Physiology: Published in Collaboration with the Entomological Society of America*, 53(4), pp.186-198.

Loeb, M.J., Martin, P.A., Hakim, R.S., Goto, S. and Takeda, M., 2001. Regeneration of cultured midgut cells after exposure to sublethal doses of toxin from two strains of Bacillus thuringiensis. *Journal of insect Physiology*, 47(6), pp.599-606.

Losick, V.P., Morris, L.X., Fox, D.T. and Spradling, A., 2011. *Drosophila* stem cell niches: a decade of discovery suggests a unified view of stem cell regulation. *Developmental cell*, 21(1), pp.159-171.

Loza-Coll, M.A. and Jones, D.L., 2016. Simultaneous control of stemness and differentiation by the transcription factor Escargot in adult stem cells: How can we tease them apart? *Fly*, 10(2), pp.53-59.

Ly, J.D., Grubb, D.R. and Lawen, A., 2003. The mitochondrial membrane potential (Δψm) in apoptosis; an update. *Apoptosis*, 8(2), pp.115-128.

MacDonald, T.T., Monteleone, I., Fantini, M.C. and Monteleone, G., 2011. Regulation of homeostasis and inflammation in the intestine. *Gastroenterology*, 140(6), pp.1768-1775.

Mantel, C., Messina-Graham, S. and Broxmeyer, H.E., 2010. Upregulation of nascent mitochondrial biogenesis in mouse hematopoietic stem cells parallels upregulation of CD34 and loss of pluripotency: a potential strategy for reducing oxidative risk in stem cells. *Cell cycle*, 9(10), pp.2008-2017.

Manzanares, M., Locascio, A. and Nieto, M.A., 2001. The increasing complexity of the Snail gene superfamily in metazoan evolution. *Trends in genetics*, 17(4), pp.178-181.

Marshman, E., Booth, C. and Potten, C.S., 2002. The intestinal epithelial stem cell. *Bioessays*, 24(1), pp.91-98.

McCurley, A.T. and Callard, G.V., 2008. Characterization of housekeeping genes in zebrafish: male-female differences and effects of tissue type, developmental stage and chemical treatment. *BMC molecular biology*, 9(1), pp.1-12.

Muratori, M., Forti, G. and Baldi, E., 2008. Comparing flow cytometry and fluorescence microscopy for analyzing human sperm DNA fragmentation by TUNEL labeling. Cytometry Part A: *The Journal of the International Society for Analytical Cytology*, 73(9), pp.785-787.

Pandey, N. and Rajagopal, R., 2017. Tissue damage induced midgut stem cell proliferation and microbial dysbiosis in *Spodoptera litura*. *FEMS Microbiology Ecology*, 93(11), p.fix132.

Parker, G.C., Acsadi, G. and Brenner, C.A., 2009. Mitochondria: determinants of stem cell fate? *Stem cells and development*, 18(6), pp.803-806.

Pauchet, Y., Muck, A., Svatoš, A., Heckel, D.G. and Preiss, S., 2008. Mapping the larval midgut lumen proteome of *Helicoverpa armigera*, a generalist herbivorous insect. *Journal of proteome research*, 7(4), pp.1629-1639.

Pfaffl, M.W., 2001. A new mathematical model for relative quantification in real-time RT–PCR. *Nucleic acids research*, 29(9), pp.e45-e45

Pinheiro, D.O., Quagio-Grassiotto, I. and Gregório, E.A., 2008. Morphological regional differences of epithelial cells along the midgut in *Diatraea saccharalis* Fabricius (Lepidoptera: Crambidae) larvae. *Neotropical Entomology*, 37(4), pp.413-419.

Rausell, C., Garcıa-Robles, I., Sánchez, J., Muñoz-Garay, C., Martınez-Ramırez, A.C., Real, M.D. and Bravo, A., 2004. Role of toxin activation on binding and pore formation activity of the Bacillus thuringiensis Cry3 toxins in membranes of Leptinotarsa decemlineata (Say). Biochimica et Biophysica Acta (BBA)-*Biomembranes*, 1660(1-2), pp.99-105.

Ravera, S., Podestà, M., Sabatini, F., Fresia, C., Columbaro, M., Bruno, S., Fulcheri, E., Ramenghi, L.A. and Frassoni, F., 2018. Mesenchymal stem cells from preterm to term newborns undergo a significant switch from anaerobic glycolysis to the oxidative phosphorylation. *Cellular and Molecular Life Sciences*, 75(5), pp.889-903.

Resende, L.P.F. and Jones, D.L., 2012. Local signaling within stem cell niches: insights from *Drosophila*. *Current opinion in cell biology*, 24(2), pp.225-231.

Roark, M., Sturtevant, M.A., Emery, J., Vaessin, H., Grell, E. and Bier, E., 1995. scratch, a pan-neural gene encoding a zinc finger protein related to snail, promotes neuronal development. *Genes & development*, 9(19), pp.2384-2398.

Robert, X. and Gouet, P. (2014) "Deciphering key features in protein structures with the new ENDscript server". Nucl. Acids Res. 42(W1), W320-W324 - doi: 10.1093/nar/gku316 (freely accessible online).

RStudio Team (2021). RStudio: Integrated Development Environment for R. RStudio, PBC, Boston, MA URL http://www.rstudio.com/

Sakakibara, S.I., Imai, T., Hamaguchi, K., Okabe, M., Aruga, J., Nakajima, K., Yasutomi, D., Nagata, T., Kurihara, Y., Uesugi, S. and Miyata, T., 1996. Mouse-Musashi-1, a neural RNA-binding protein highly enriched in the mammalian CNS stem cell. *Developmental biology*, 176(2), pp.230-242.

Sangiorgi, E. and Capecchi, M.R., 2008. Bmi1 is expressed in vivo in intestinal stem cells. *Nature genetics*, 40(7), pp.915-920.

Santos, C.D., Ribeiro, A.F., Ferreira, C. and Terra, W.R., 1984. The larval midgut of the cassava hornworm (*Erinnyis ello*). *Cell and Tissue Research*, 237(3), pp.565-574.

Savignan, F., Ballion, B., Odessa, M.F., Charveron, M., Bordat, P. and Dufy, B., 2004. Mitochondrial membrane potential (DeltaPsi) and Ca2+-induced differentiation in HaCaT keratinocytes. *Journal of biomedical science*, 11(5), pp.671-682.

Scaduto Jr, R.C. and Grotyohann, L.W., 1999. Measurement of mitochondrial membrane potential using fluorescent rhodamine derivatives. *Biophysical journal*, 76(1), pp.469-477.

Schieke, S.M., Ma, M., Cao, L., McCoy, J.P., Liu, C., Hensel, N.F., Barrett, A.J., Boehm, M. and Finkel, T., 2008. Mitochondrial metabolism modulates differentiation and teratoma formation capacity in mouse embryonic stem cells. *Journal of Biological Chemistry*, 283(42), pp.28506-28512.

Scoville, D.H., Sato, T., He, X.C. and Li, L., 2008. Current view: intestinal stem cells and signaling. *Gastroenterology*, 134(3), pp.849-864.

Sukumar, M., Liu, J., Mehta, G.U., Patel, S.J., Roychoudhuri, R., Crompton, J.G., Klebanoff, C.A., Ji, Y., Li, P., Yu, Z. and Whitehill, G.D., 2016. Mitochondrial membrane potential identifies cells with enhanced stemness for cellular therapy. *Cell metabolism*, 23(1), pp.63-76.

Tabashnik, B.E., 1994. Evolution of resistance to Bacillus thuringiensis. *Annual review of entomology*, 39(1), pp.47-79.

Tabashnik, B.E., Brévault, T. and Carrière, Y., 2013. Insect resistance to Bt crops: lessons from the first billion acres. *Nature biotechnology*, 31(6), pp.510-521.

Takashima, S. and Hartenstein, V., 2012. Genetic control of intestinal stem cell specification and development: a comparative view. *Stem Cell Reviews and Reports*, 8(2), pp.597-608.

Tettamanti, G., Grimaldi, A., Casartelli, M., Ambrosetti, E., Ponti, B., Congiu, T., Ferrarese, R., Rivas-Pena, M.L., Pennacchio, F. and Eguileor, M.D., 2007. Programmed cell death and stem cell differentiation are responsible for midgut replacement in Heliothis virescens during prepupal instar. *Cell and tissue research*, 330(2), pp.345-359.

Whiteley, M., Noguchi, P.D., Sensabaugh, S.M., Odenwald, W.F. and Kassis, J.A., 1992. The *Drosophila* gene escargot encodes a zinc finger motif found in snail-related genes. *Mechanisms of development*, 36(3), pp.117-127.

Wu, K., Yang, B., Huang, W., Dobens, L., Song, H. and Ling, E., 2016. Gut immunity in Lepidopteran insects. *Developmental & Comparative Immunology*, 64, pp.65-74.

Ye, X.Q., Wang, G.H., Huang, G.J., Bian, X.W., Qian, G.S. and Yu, S.C., 2011. Heterogeneity of mitochondrial membrane potential: a novel tool to isolate and identify cancer stem cells from a tumor mass? *Stem Cell Reviews and Reports*, 7(1), pp.153-160.

Young, R.A., 2011. Control of the embryonic stem cell state. *Cell*, 144(6), pp.940-954.

Zhang, P. and Turnbull, M.W., 2018. Virus innexin expression in insect cells disrupts cell membrane potential and pH. *Journal of General Virology*, 99(10), pp.1444-1452.

Zhang, S., Xu, Y., Fu, Q., Jia, L., Xiang, Z. and He, N., 2011. Proteomic analysis of larval midgut from the silkworm (*Bombyx mori*). *Comparative and functional Genomics*, 2011.

Zhou, Y., Jia, B., Han, L. and Peng, Y., 2019. Morphological and functional characterization of isolated stem cells from the midgut of *Chilo suppressalis* larvae. *Journal of Asia-Pacific Entomology*, 22(3), pp.982-989.